Major Project

Dissertation on

"COMPUTATIONAL ANALYSIS OF WEAR BEHAVIOUR ON PIN ON DISC SETUP FOR THERMAL SPRAY OF COATING USING ANSYS"

Submitted to Delhi Technological University in partial fulfillment of the requirement for the award of Degree of

Master of Technology

In

Computational Design

SONU NAVGOTRI

2K13/CDN/15

UNDER THE SUPERVISION OF

Dr. R.S.WALIA   Dr. MOHIT TYAGI

Associate Professor   *Assistant Professor*

Department of Mechanical Engineering
Delhi Technological University
(Formerly Delhi College of engineering)
Bawana Road, Delhi-110042

JULY 2015

CERTIFICATE

DELHI TECHNOLOGICAL UNIVERSITY
(Formerly DELHI COLLEGE OF ENGINEERING)

Date:-_____

This is to certify that report entitled **"COMPUTATIONAL ANALYSIS OF WEAR BEHAVIOUR ON PIN ON DISC SETUP FOR THERMAL SPRAY OF COATING USING ANSYS"** by **SONU NAVGOTRI** is the requirement of the partial fulfillment for the award of Degree of **Master of Technology (M. Tech)** in **Thermal Engineering** at **Delhi Technological University**. This work was completed under my supervision and guidance. He has completed her work with utmost sincerity and diligence. The work embodied in this project has not been submitted for the award of any other degree to the best of my knowledge.

Dr. R.S. WALIA   **Dr. MOHIT TYAGI**

Associate Professor   **Assistant Professor**

(SUPERVISIOR)   **(SUPERVISOR)**

Department of Mechanical Engineering   **Department of Mechanical Engineering**

DELHI TECHNOLOGICAL UNIVERSITY   **DELHI TECHNOLOGICAL UNIVERSITY**

ACKNOWLEDGEMENT

First of all, I would like to express my gratitude to God for giving me ideas and strengths to make my dreams true and accomplish this thesis.

To achieve success in any work, guidance plays an important role. It makes us put right amount of energy in the right direction and at right time to obtain the desired result. Express my sincere gratitude to my guide **Dr. R. S. WALIA** Associate Professor, and **Dr. MOHIT TYAGI** Assistant Professor, Mechanical Engineering Department for giving valuable guidance during the course of this work, for his ever encouraging and timely moral support. His enormous knowledge always helped me unconditionally to solve various problems.

I am greatly thankful to **Dr. R. S. MISHRA**, Professor and Head, Mechanical Engineering Department, Delhi Technological University, for his encouragement and inspiration for execution of the this work. I express my feelings of thanks to the entire faculty and staff, Department of Mechanical Engineering, Delhi Technological University, and Delhi for their help, inspiration and moral support, which went a long way in the successful completion of my report work.

SONU NAVGOTRI

(Roll No-2K13/CDN/15)

[ii]

ABSTRACT

Tribological simulation can be seen as a new study problem developed from modern information technology and computer simulation technology in combination with a variety of mathematical methods in the field of tribology. Due to the complexity of actual tribological systems and different working conditions, the results obtained from traditional simulation test method were often qualitative only, and couldn't be used in designing of tribological systems and practical engineering applications. There is a need to seek new ways and means of in-depth study of the wear quantitative law, otherwise the fundamental breakthrough of the prevention and control of the wear could not be achieved. The tribological simulation research of the typical pin on disc sliding wear test system was carried by the adoption of computer technology and mathematical analysis methods in order to provide a new wear analysis method for the simulation of the basic tribological contact problems.

In this research work, the wear simulation model including multiple parameters was established based on experimental data and theoretical data. The parameters of the model were determined by the test data. The simulation model reflects the basic relationship between input and output of the pin on disc dry sliding wear test. Simulation results shows that as the load on pin increase depth wear also increase with angular velocity remains the same .And it also reveals the effect of pin diameter on wear depth.

Keywords: Thermal spray of coating, wear, ANSYS, tribology, finite element method.

CONTENTS

LIST OF FIGURES

LIST OF TABLE

ACRONYMS

Acronym	Description
PoD	Pin on Disc
CoF	Coefficient of friction
BC	Boundary conditions
FEM	Finite element method
ASTM	American Society for Testing and Materials
DOF	Degree of freedom
CPRESS	Contact pressure

CHAPTER 1

INTRODUCTION

The subject of Tribology requires a diverse knowledge base from many different scientific specialties. Students of the subject can gain immense satisfaction from tackling problems requiring the application of fundamental concepts rooted in the traditional studies of science and engineering, yet it is difficult within the existing schemes of study for anyone to feel fully in command of a subject dealing with interacting surfaces. Tribology involves a significant amount of experimental science. In the past, progress has usually been preceded by some experiment or experimental observation. One of the foremost reasons for the lack of concrete finite element modeling is that a tribosystem is made up many different variables such as contract stress, surface roughness, sliding speed, chemical environments, temperature, humidity, material type, among others. Any modification in the combination of these variables may yield completely different test results.

Two of the most widely used measures to characterize the performance of a tribosystem are friction and wear. Both friction and wear data can be highly informative to engineers and materials scientists in order to designing and evaluating an engineering system. Bayer made the observation that there tends to be a tendency to assume linear relationships between wear when extrapolating design for a tribosystem. Due to the complex nature of wear phenomena, such relationships are often nonlinear and have varying nature between tribosystem. It has been clear from the previous research that friction and wear are chaotic processes; however it is possible to model the contact behavior between two materials.

The key objective of tribology is to minimize the friction and wear problem of solid-to-solid contact. This statement is quite inaccurate; in automotive tires one wishes to maximize the friction and minimize the wear. During the break in period of an internal combustion engine, one wishes to maximize friction and wear of the piston rings and for proper seating and sealing. Finally, in the application of wax to the bottom surface of a snowboard, one wishes to minimize friction and maximize wear as to impart as much wax as possible while doing as little work as possible.

Tribology deals with the synergy of any natural or engineered systems that have two pairs, liquid or solid, in contact with each other. The relative motion between these pairs makes it impossible

to directly observe and predict the behavior of contact. There are tremendous challenges and areas to be explored.

1.1 Tribology: A short history

The history of any modern-day science is often quite rich. Historical evidence is found through archaeological fact and occasional written record. The history of tribology is no different, with tribological achievements spanning the time from the beginning of mankind, to modern day. The field of tribology is relatively more important, it was invented in 1966 by British physicist David Tabor. The practice and fundamental aspects of Tribology are quite old. The root word "tribos" is translated from Greek to mean "rubbing", and many early important tribological observations were made by Greek philosophers, scientists, and mechanicians. For example, in 400 B.C., Aristotle made the observation in his work *Questions Mechanicae* that friction was known as a very perceptible force and minimum for round objects. Table 1.1 below highlights a few of the historical achievements in tribology pertinent to this research.

1.2 Tribotesting

The development of the standardization of tribological research and experimentation was a result from a 1966 report prepared by the British Lubrication Engineering Working Group entitled *Lubrication (Tribology) Education and Research – A report on the Present Position and Industry's Needs*. The report outlined significant deficiencies concerning tribological education and research; and the practical application of the science to large industry. One of biggest driving goals in the development of tribological science was an economic one. As an example, it was found that the potential savings to British industry resulting from improvements in education and research were about £515 million per annum.

Since the British Working Group published the famous 1966 report, many of the developments in tribological testing have been driven by industry in order to evaluate the performance of machines and machine elements like: gears, bearings (roller, ball, journal, air, etc.), valves, and lubricants. Many of the testing methods have now been standardized and are governed by strict ASTM standards. A sample of the more than one hundred ASTM standards for testing friction and wear are shown in table 1.2.

Table 1.1: History of important tribological achievements

Tribologist	Achievement	Time Period
Early mankind	Earliest use of friction in conquest of fire through rubbing, drilling, or percussion.	c. 1,000,000-11,000 years ago
Egyptian Civilization	Transport of 500 ton obelisks on sledges	c. 2400 B.C.
Greek and Romans	Focus on philosophy and science by Greek and roman cultures, use of metal bearings and lubricant.	c. 900 B.C. – A.D. 400
Leonardo da Vinci	Observation of proportionality of friction. Wear studies for development of bearing materials. Invention of rolling element bearings.	c. 1400-1600
Guillaume Amontons Charles Augustin Coulomb Leonhard Euler	Development of Laws of Friction. Coefficient of friction defined.	c. 1600-1750
Heinrich Hertz	Development of elastic body contact theory over Christmas vacation at the age of 23.	1881

Table 1.2: ASTM standards for testing friction and wear.

ASTM Standard	Title	Parameters Measured
G99 – 05	Standard Test Method for Wear testing with a Pin-on-disk Apparatus	Volumetric wear loss
D 2981 – 94	Test Method for Wear Life of Solid Film Lubricants in Oscillation Motion	Coefficient of friction and wear at failure
D913 – 03e1	Standard Test Method for Evaluating Degree of Resistance to Wear of Traffic Paint	Degree of substrate coverage over area of representative wear
B611 – 85	Standard Test Method for Abrasive Wear Resistance of Cemented Carbides	Abrasion resistance and wear number
D3702 – 94	Standard Test Method for Wear Rate and Coefficient of Friction of Materials in Self-Lubricated Rubbing Contact Using a Thrust Washer Testing Machine	Wear rate and coefficient of friction

The objective of most tribological testing is to emphasize the frictional power values and to measure the wear values for wear system. With a specific end goal to completely comprehend the rubbing and wear values, the parameters used to portray grinding and wear must be caught on. This is discriminating when looking at qualities from changed studies and testing routines. The parameters apropos to this exploration will be examined inside and out beneath.

1.3 Friction parameters

The well known study in the subject of misfortunes credited to contact was distributed by French researcher Guillaume Amontons in 1699. The consequences of Amontons' work with friction are known as the laws of friction, point by point beneath:

1. The power of friction is straightforwardly relative to the connected burden.

2. The power of friction is free of the clear range of contact.

Through the extra work in grating study by Charles Augustin Coulomb and Leonhard Euler the amount of friction in contacting bodies is alluded to as the coefficient of friction as given in equation 1.

$$\mu = \frac{F}{N} \tag{1.1}$$

Where:

F denotes frictional force acting tangential to the contact surface [N]

N denotes the normal force acting normal to the contacting surface [N]

μ denotes the coefficient of friction between the two bodies.

1.4 Hertzian contact pressure

Mechanics of materials tell us that two solid bodies in contact will deform under an applied load. This deformation will either be elastic or plastic, depending on the magnitude of the applied load and materials in contact. In many tribological applications, such as bearings, the surfaces are non-conformal and the contact areas are very small and resulting pressures very high. Using relationships developed by Hertz, based on the theory of elasticity, the stress at the point of contact of the materials can be calculated. The maximum contact pressure between two bodies is often referred to as the Hertzian contact pressure. The Hertzian contact pressure is a function of the contact area 'A', and normal load 'W', reduced contact radius 'R', and reduced Young's modulus 'E'.

The relationship between these values for the standard pin-on-disk geometry in which the pin is spherical and the sample surface flat is detailed in the equations 1.2 to 1.5. These equations are valid for all experiments performed in this research work for pin-on-disk configuration under a pure sliding condition. The reduced radius of curvature for contact between a sphere and flat surface is shown in equation 1.2 as given below:

$$\frac{1}{R'} = \frac{2}{R_A} \tag{1.2}$$

Where:

R´ denotes the reduced radius of curvature [m]

R_A denotes the radius of the sphere [m]

The reduced Young's modulus is defined as:

$$\frac{1}{E'} = \frac{1}{2}\left[\frac{1-v_A^2}{E_A} + \frac{1-v_B^2}{E_B}\right] \tag{1.3}$$

Where:

E´ denotes the reduced Young's modulus [Pa]

v_A denotes the Poisson's ratio of the sphere material

v_B denotes Poisson's ratio of the sample material

E_A denotes Young's modulus of the sphere material [Pa]

E_B denotes Young's modulus of the sample material [Pa].

The contact area radius between pin and sample for the given geometry is calculated using equation 1.4 as given below:

$$a = \left(\frac{3WR'}{E'}\right)^{1/3} \tag{1.4}$$

Where:

a denotes the radius of contact area [m]

W denotes the normal load [N]

R' denotes the reduced radius of curvature [m]

E' denotes the reduced Young's modulus [Pa]

[6]

In tribologilical studies, the diameter of the contact area 2a, is called the semi-contact width.

The maximum Hertzian contact pressure can be calculated from equation 1.5 given below:

$$P_{max} = \frac{3W}{2\pi a^2}$$ (1.5)

Where:

P_{max} denotes the maximum Hertzian contact pressure [Pa].

1.5 Wear

Wear of materials can be defined as a progressive damage to a surface caused by relative motion with respect to another substance. This broad definition of wear is meant to include traditional aspects like loss of volume in a material as well as non-tradition aspects like dimensionality change though plastic deformation and surface and subsurface cracking. There are three different ways in which wear maybe classified. The first one is in terms of the wear scar present after testing. Examples of terms used to classify the wear scar are pitted, ploughed, scratched, grooved, gouged, and such. The second classification is in terms of the characteristic type of wear mechanisms. The most prevalent being adhesion, abrasion, and oxidative type wear. The third method to classify wear is in terms of wear in an engineered or test system. Many examples such as lubricated wear, non-lubricated wear, pure sliding wear, and rolling wear were used by field experts (engineers). In the present research work, all three categories have been used to describe the type of wear present. To understanding wear mechanisms between solids is critical for an engineer as it can often influence friction behavior and induce failure. For this reason a brief explanation of wear mechanisms will be given below.

1.5.1 Adhesive wear

There have not been any predictive theories quantitatively confirmed by experts for the adhesive wear of ductile materials. The highest values of adhesion are often seen for a combination of like metals, but are common in all metal-to-metal contacts. Additionally, high values of adhesion have been reported between metals and polymers, and metals and ceramics. Transfer films are the most characteristic features of adhesion, and occur when material is transferred from one surface to another. This is most evident by areas in which material has delaminated from one

contacting surface. Transfer films can also appear as highly plastically deformed wear particles. Surface cracks are also evident of severe adhesive wear.

1.5.2 Abrasive wear

Wear by abrasion is wear caused by contact between a particle and solid material. It is typically caused when the hardness of the two testing materials vary. Hard wear particles or asperities from one surface are moved through the softer surface by the relative motion between bodies. Abrasion happens though cutting, fracture, and fatigue. Cutting is most commonly seen in ductile materials and is thought of as a sharp "grit" or hard asperity cutting the softer surface. The cut material is removed as wear debris. Cutting can take the form of micro cutting by small hard grits or "ploughing" of larger grits through the surface. Fracture is typically found in brittle materials in which the contact with sharpened grits causes crack formation and growth. This build up in cracking ultimately leads to the release of large quantities of material through fracture of the wear surface. Fatigue is caused by repeated strain caused by grits deforming the area on the surface. Abrasive wear happens by two modes; two-body, and three-body. Two-body abrasive wear is similar to the use of sandpaper on a surface. In which the wear producing agent is the counter surface. This is usually done through hardened grits or asperities. In three-body abrasive wear the grits are allowed to freely roll and slide over the surface.

1.5.3 Oxidative wear

An oxide film is present on almost all metals and also appears on any clean surface exposed to oxygen even at cryogenic temperatures. At high sliding speeds, oxidative wear is caused by the rapid oxidation of the metallic testing surface due to high temperatures created by friction heating between the two surfaces. Oxide layers at the highest contact spots are continuously built up and destroyed. At high sliding speeds, oxide films of several micrometers thick can build up on the worn surface. At lower sliding speeds frictional temperature rises are not high enough to causes rapid oxidation at asperity tips. Oxidative wear is still prevalent due to the accreditation of pre-existing surface oxide wear debris in the worn surface.

1.6 Wear parameters

To categorize varying levels of wear experienced at different test parameters between the surfaces of solids, a wear parameter must be defined. For this purpose the specific wear rate, k will be defined in the expression below.

$$k = \frac{V}{W \times L} \tag{1.6}$$

Where:

k denotes the specific wear rate [m^3/Nm]

V denotes the wear volume [m^3]

W denotes the normal load [N]

L denotes the total sliding distance [m].

1.7 Pin on disc Test

When surfaces are in contact they usually transmit shear as well as normal forces across their interface. There is generally a relationship between these two force components. This relationship known as the friction between the contacting bodies, is usually expressed in terms of the stresses at the interface of the bodies. With a Pin on Disc (PoD) test rig the CoF between two materials can be determined. Before modeling an ABAQUS-model one has to understand what the theory is behind the PoD- test. Therefore the Coulomb friction model theory will be explained. The real Coefficient of friction (CoF) consists of two separated CoF's, namely the static and dynamic CoF. They have both their own region in which they are valid. When there is no slip (no movement between the contacting surfaces), the static CoF is valid. When the slip is infinite the dynamic CoF is valid, see figure 1.1. In between there is transition region. The transition from static to dynamic friction results in a small startup error after that there is no linear behavior. Then the dynamic CoF becomes constant. In case of a fixed normal force, the reaction force of the static CoF is not constant. It is dependent on the magnitude of the applied force and can be calculated with equation 1.1, it has a linear behavior. The transition from the static to the dynamic friction has in the beginning a small startup error and then becomes

constant and can be determined with the same equation, equation 1.7. The net force, which is available for the movement can be calculated with equation1.8.
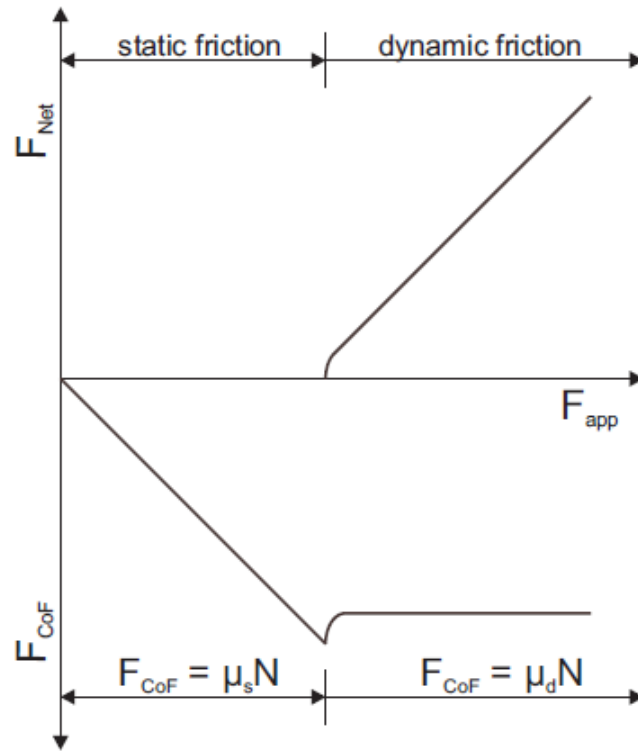
Figure 1.1a: Static and dynamic friction forces
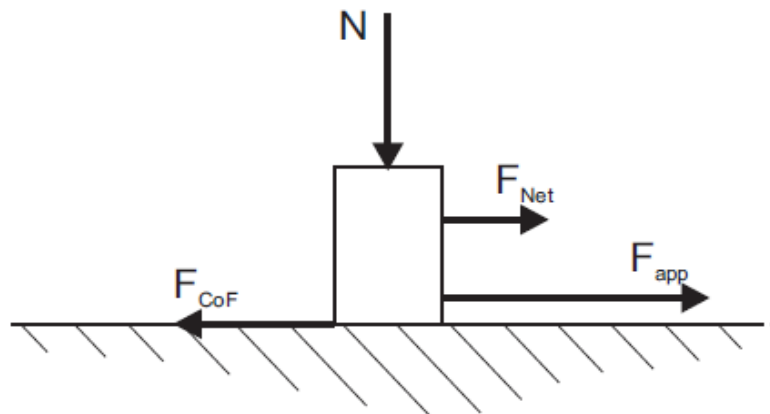
Figure 1.1b: Frictional forces.

$$F_{CoF} = N.\mu \tag{1.7}$$

$$F_{net} = F_{app} - F_{CoF} \tag{1.8}$$

In figure 1.2 the forces that are acting in the PoD-test are presented. At the top of the pin, a force normal force N is applied. The disc is rotating with a fixed speed 'ω'. Due to the normal force, the angular speed and the F_{CoF} a reaction force will occur. This reaction force is the friction force F_{CoF} . The force that is applied at the disc surface F_{app}, is the opposite of this force and is F_{CoF} . The torque force, F_T , is the same as the applied force, F_{app}, equation 1.8. This force is larger than the friction force and can be compared with the applied force, equation 1.9. The force that is acting on the disc is dependent of the radius on which the pin is acting, equation 1.10. The power needed to drive the disc is the torque multiplied with the angular velocity, equation 1.11.

$$F_T = F_{app} \tag{1.9}$$

$$T = F_T.r \tag{1.10}$$

$$P = T.\omega \tag{1.11}$$

Figure 1.2: Forces acting on pin on disc test

[11]

1.8 Thermal spray coatings

Thermal spraying techniques are coating processes in which melted (or heated) materials sprayed onto a surface. The "feedstock" (coating precursor) is heated by electrical (plasma or arc) or chemical means (combustion flame).

Thermal spraying can provide thick coatings (approx. thickness range is 20 micrometers to several mm, depending on the process and feedstock), over a large area at high deposition rate as compared to other coating processes such as electroplating, physical and chemical v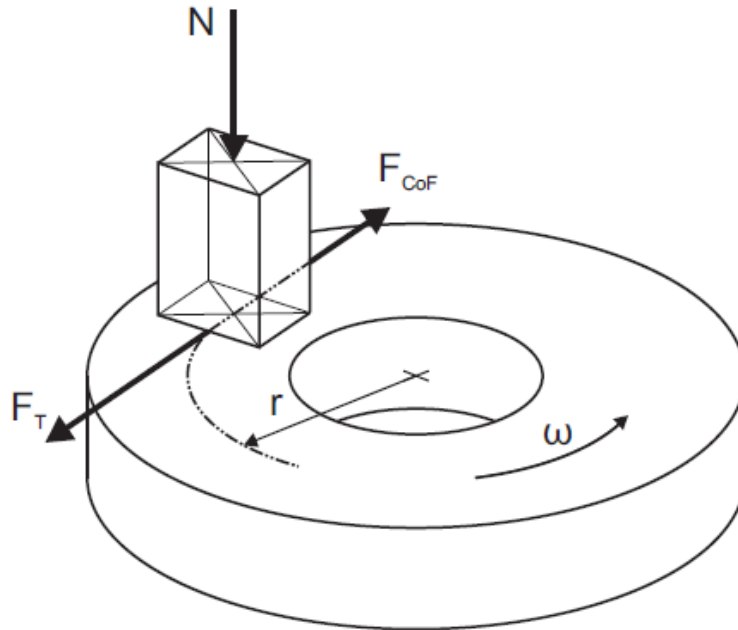apor deposition. The coating material of thermal spraying includes metals, alloys, ceramics, plastics and composites. They are fed in powder or wire form, heated to a molten or semi molten state and accelerated towards substrates in the form of micrometer-size particles. Combustion or electrical arc discharge is usually used as the source of energy for thermal spraying. Resulting coatings are made by the accumulation of numerous sprayed particles. The surface may not heat up significantly, allowing the coating of flammable substances.

Coating quality is usually assessed by measuring its porosity, oxide content, macro and micro-hardness, bond strength and surface roughness. Generally, the coating quality increases with increasing particle velocities.

1.9 Finite Element Method

The finite element method as we know it today seems to have originated with Courant in 1943. Courant determined the torsional rigidity of a hollow shaft by dividing the cross-section into triangles and interpolating a stress function φ linearly over each triangle from the values of φ at nodes. The name finite element was coined by Clough in 1960. Many new elements for stress analysis were soon developed. In 1963, finite element analysis acquired respectability in academia when it was recognized as a form of the Rayleigh-Ritz method. Thus finite element analysis was seen not just as a special trick for stress analysis but as a widely applicable method having a sound mathematical basis. The first textbook about finite element analysis appeared in 1967 and today there exist an enormous quantity of literature about finite element analysis.

General-purpose computer programs for finite element analysis emerged in the late 1960's and early 1970's. Since the late 1970's, computer graphics of increasing power have been attached to finite element software, making finite element analysis attractive enough to be used in actual design. Previously it was so tedious that is was used mainly to verify a design already completed or to study a structure that had failed. Computational demands of practical finite element analysis are so extensive that computer implementation is mandatory. Analyses that involve more than 100 000 degrees of freedom are not uncommon.

Finite element analysis, also called the finite element method, is a method for numerical solution of field problems. A field problem requires determination of the spatial distribution of one or more dependent variables. Mathematically, a field problem is described by differential equations or by an integral expression. Either description may be used to formulate finite elements.

Individual finite elements can be visualized as small pieces of a structure. In each finite element a field quantity is allowed to have only a simple spatial variation, e.g. described by polynomial terms up to x^2, xy and y^2. The actual variation in the region spanned by an element is almost certainly more complicated, hence a finite element analysis provides an approximate solution.

In more and more engineering situations today, we find that it is necessary to obtain approximate numerical solutions to problems, rather than exact closed-form solutions.

Elements are connected at points called nodes and the assemblage of elements is called a finite element structure. The particular arrangement of elements is called a mesh. How the finite element method works can be summarized in the following general terms.

1. **Discretise the continuum**. The first step is to divide the continuum or solution into elements. A variety of element shapes may be used and different element shapes may be employed in the same solution region.

2. **Select interpolation functions**. The next step is to assign nodes to each element and then choose the type of interpolation function to represent the variation of field variable over the element.

3. **Find the element properties**. Once the finite element model has been established the matrix equation expressing the properties of the individual elements is ready to be determined.

4. **Assemble the element properties to obtain the system equations**. The matrix equations expressing the behavior of the elements must be combined to form the matrix equations expressing the behavior of the entire solution region or system.

5. **Solve the system equations.** The assembly process of the preceding step gives a set of simultaneous equation that can be solved to obtain the unknown nodal values of the field variable.

Finite element analysis has advantages over most other numerical analysis methods, including versatility and physical appeal. The major advantages of finite element analysis can be summarized as:

- Finite element analysis is applicable to any field problem.

- There is no geometric restriction. The body analyzed may have any shape.

- Boundary conditions and loading are not restricted.

- Material properties are not restricted to isotropy and may change from one element to another   or even within an element.

- Components that have different behaviors, and different mathematical descriptions, can be combined.

- A finite element analysis closely resembles the actual body or region.

- The approximation is easily improved by grading the mesh.

Some disadvantages may be mentioned as well:

- It is fairly complicated, making it time-consuming and expensive to use.

- It is possible to use finite element analysis programs while having little knowledge of the analysis method or the problem to which it is applied. Finite element analyses carried out without sufficient knowledge may lead to results that are worthless and some critics say that most finite element analysis results are worthless.
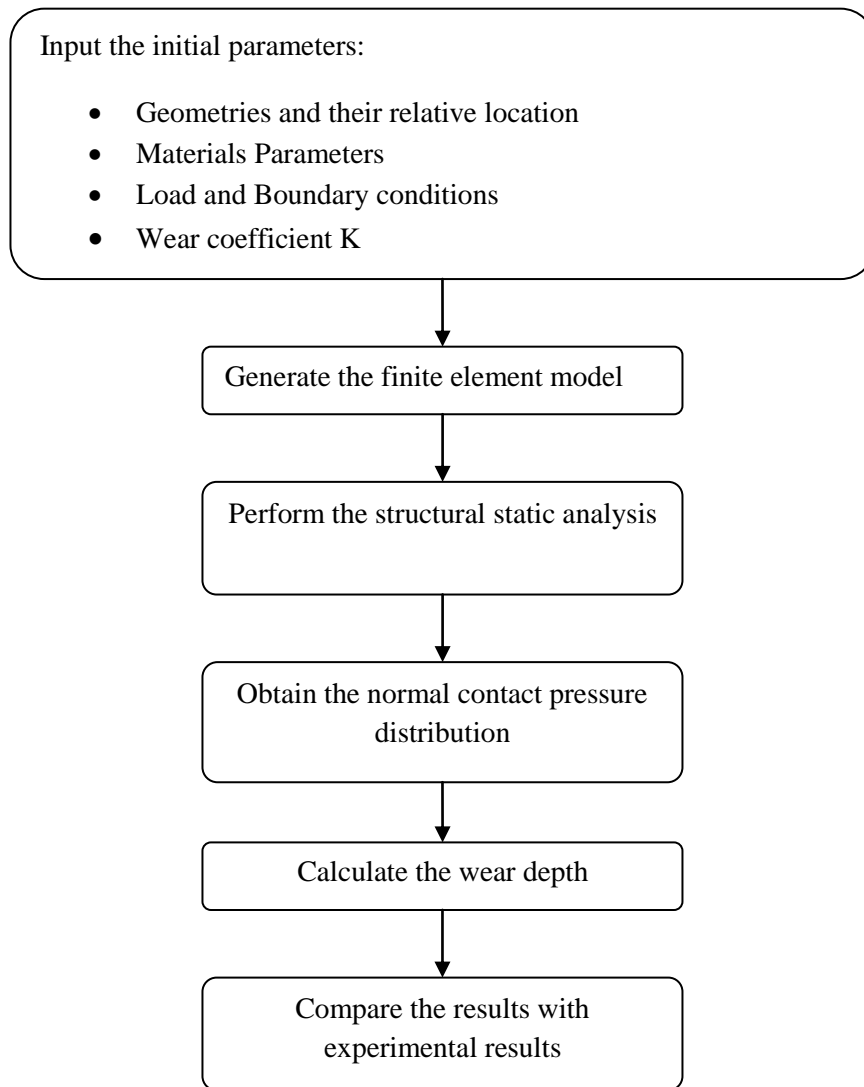
Figure 1.3: Finite element wear simulation approach.

1.10 The Archard Equation

The starting point for any discussion of wear on the macro scale is the Archard equation (Podra and Anderson, 1999) [13], which states that:

$$W = K \times S \times P \tag{1.12}$$

Where,

W denotes the worn volume,

K denotes the wear per unit load per sliding distance and

S denotes the sliding distance,

P denotes the contact pressure between the sliding surfaces.

According to Archard (1866) 'K' may be described as the coefficient of wear and, in a series of experiments with the same combination of materials; changes in 'K' denote changes in surface conditions. The Archard equation assumes that the wear rate is independent of apparent area of contact. However, it makes no assumptions about the surface topography (surface roughness effects are encompassed by the experimental wear coefficient) and it also makes no assumptions about variations with time. It must also be stated that although it is widely used, the Archard equation only provides for an order of magnitude estimate and is a true calculation of wear. One of the more common methods for determining the value for 'K' is to press a stationary pin using a preload of 'P' into the surface of a rotating disk. The load 'P' is known and the sliding distance 'S' can be determined from the rotational speed of the disk and time that the disk has rotated. The amount of wear on the pin is determined by change in mass (weight) of the pin and the constant 'K' calculated. This method for determining a constant wear coefficient for a given pair of surfaces has limitations. It ignores changes in apparent area of contact with time, also known as "running in" effects. It assumes that the direction of the load is constant, which may not be the case in real conditions. It assumes that the surface topography of the experimental surfaces accurately represent the surfaces of interest.

Despite of these limitations, it will be assumed that the values of wear coefficients determined by the pin on disc method or by other methods are accurate enough to use in engineering analysis.

In this research work value of specific wear rate 'K' is obtain form the experimental results of pin on disc test using hard chrome disc and cylinder liner pin.

1.11 ANSYS Software Package

ANSYS is developed by Dr. John A. Swanson, Inc [01]. It is a complete package of powerful engineering simulation programs, based on the finite element method. This simulation software is capable of performing simple linear analysis to the most complex nonlinear simulations.

With the development of computer technology, attention in solution of contact problems has shifted from traditional analytic solution towards finite element analysis (FEA). As it is well known, ANSYS can be applied in structure and non-linearity coupled-field, etc. For contact

problems, ANSYS can model contact condition with contact element and present Lagrange multiplier, penalty function and direct constraint approach.

1.12 Contact Interaction

Since Indentation is an example of typical contact problem, it is very important to define the contact formulation in ANSYS. In general the interaction between contacting surfaces consists of two components: one normal to the surfaces and one tangential to the surfaces. The normal component may be referred as contact pressure and the tangential component generates the relative motion (sliding) of the surfaces involving friction. ANSYS uses Coulomb friction model to define the interaction of contacting surfaces. The model characterizes the friction behavior between the surfaces using a coefficient of friction 'µ'. The product µ×P, where P is the contact pressure between the two surfaces, gives the limiting frictional shear stress. The contact surfaces will not slip (sliding relative to each other) until the shear stress across their interface equals the limiting frictional shear stress, µ×P.

In this research work friction effect is considered due to the interaction of pin and disc. The interaction between the indenter and the specimen is modeled as contact pair with friction. According to ANSYS user manual [01], the indenter surface is defined as the 'master' surface since the indenter is rigid body. The top of the specimen is the 'slave' surface.

CHAPTER 2

<u>LITERATURE REVIEW</u>

2.1 FEM literature

Podra and Andersson, (1999) [02] have studied the wear simulation approach with commercial finite element software ANSYS. A modeling and simulation procedure was proposed and used with the linear wear law and the Euler integration scheme. A spherical pin on- disc unlubricated steel contact was analyzed both. Experimentally and with finite element method (FEM), and the Lim and Ashby wear map was used to identify the wear mechanism. It was shown that the FEA wear simulation results of a given geometry and loading can be treated on the basis of wear coefficient-sliding distance change equivalence. The finite element software ANSYS was well suited for the solving of contact problems as well as the wear simulation. The actual scatter of the wear coefficient was within the limits of 40-60% led to considerable deviation of wear simulation results. Due to the model simplifications and the real deviation of input data, the FEA wear simulation results was evaluated on a relative scale to compare different design options, rather than to be used to predict the absolute wear life.

Kim et al. (2005) [03] have proposed a numerical approach that simulates the progressive accumulation of wear in oscillating metal on metal contacts. The approach used a reciprocating pin-on disk tribometer to measure a wear rate for the material pair of interest. This wear rate was an input to a FEA that simulates a block-on-ring experiment. After the simulation, two block-on-ring experiments were performed with the same materials that were studied in the reciprocating pin-on-disk experiments. The results from the FEA were in close agreement with the block on-ring experimental results. This approach did not either rely on curve fitting or use the block-on-ring experimental data as model inputs. The FEA were performed by progressively changing nodal coordinates to simulate the removal of material that occurs during surface interaction. The continuous wear propagation was discretized and an extrapolation scheme was used to reduce computational costs of this simulation.

Zhang and Meng, (2006) [11] have proposed a linear sliding wear model with ratcheting effects to describe the wearing process and a simplified mathematical method was presented to simulate the wear of the rotor bushing sliding on the ground plane. The effects of geometry parameters,

material properties and applied operating conditions on the evolution of dimensional and volumetric wear rates were explored for normally loaded rotating rotor bushing sliding on the ground plane. The hemispherical-bushing-on-ground plane configuration finite element model was established and the implementation of the contact problem based on ANSYS finite element software and contact element approach was introduced to investigate contact problems in micro motors. Numerical simulations and results of the contact stresses and contact pressure were studied and the effects of wear coefficient, material selections, surface roughness and geometry structures, etc., were discussed in detail. It was indicated that the non-linear effects could not be ignored and these results must be evaluated on a relative scale to compare different design options.

2.2 Coating literature

Bosman et. al. (2012) [04] predicted a mild wear map for boundary lubricated contacts is presented and validated using model experiments. Both the transition from mild to severe wear as mild wear itself is modelled. The criterion for the transition from mild to severe wear is a thermal one. The mild wear model is based on the hypothesis that for an additive to protect the surface against severe wear a sacrificial chemical layer should be present at the surface.

Wear map of grey cast iron is reported by **Riahi et. al. (2003)** [05] to summarize wear rate and its mechanism of A30 grey cast iron against AISI 52100 type steel at load of 0.3-50.0 N and sliding range of 0.2-3.0 m/s. Ultra mild wear at a rate of 8×10^{-7} and 9×10^{-7} mm^3/m at 0.3 N for 0.2 and 0.5 m/s. In mild wear regime rage of wear rate 10^{-5} mm^3/m at low loading condition, and 10^{-4} mm^3/m at high operating condition. Severe wear regime shows the rate of 10^{-1} to 3.2×10^{-1} mm^3/m compared to those of mild regime.

Wear maps for titanium nitride coatings deposited on copper and brass a widely used group of engineering materials in numerous applications reported by **Subramanian et. al. (2000)** [06] shows the coefficient of friction increases with the increase in the thickness of electroless nickel (EN) interlayer for both copper and brass substrates. Scratch adhesion tests were performed and the results interpreted via a profilometer and microscopic examination. Recommendations have been made as to appropriate nickel interlayer thicknesses for a given degree of wear resistance as reflected in the coating failure mechanism, by way of the so-called wear map.

Friedrich et. al (1997) [07] Studied tribological behaviour of chromium nitride (CrN) deposited by RF magnetron sputtering. Mechanical properties like hardness, residual stress, adhesion and thickness are used for characterization. Sliding kinematics is used to understand the contact mechanics of tribological system at high loading condition at the range of 7 mm thickness. Result shows the moderate residual stress and surface adhesion from the substrate followed by reducing wear rate comparison to uncoated material in tribological application.

Broszeit et. al. (1999) [08] investigated the deposition and application of CrN coating deposited by physical vapour deposition (PVD) and discussed the problems associated with chromium (Cr) electroplating and behaviour of titanium nitride (TiN) which are not up to the mark with various process parameters. CrN is one of the answers of these problems suggested by author. Coating thickness of CrN slightly decreases by increasing the temperature while thickness of TiN increase at elevated temperature. Electroplated chromium (Cr) shows highest deposition rate but deposition rate of TiN and CrN, chromium nitride shows higher deposition rate. It replaces the TiN and electroplating of Cr with their promising corrosion resistance and several applications. Titanium (Ti) alloy against alumina-bronze 630 is reported by M.Y.P.

Costa et. al. (2010) [09] investigated that the high velocity oxygen fuel (HVOF) WC–10%Co–4%Cr thermal sprayed and TiN, CrN and DLC physical vapour deposition (PVD) coatings were applied to increase titanium substrate wear and friction resistance. Quantitative comparison was done at force of 5N and speed of 0.5m/s at various co0ndition.Graphite carbon structures for Ti–6Al–4V alloy DLC coated and aluminium–bronze 630 tribological pair works as a solid lubricant to prevent the wear.

According to the need of industrial application; **Navinsek et. al. (1997)** [10] studied single layer, low and high temperature CrN coatings and double TiN + CrN coatings. CrN PVD coatings deposited at 450°C high temperature and 250°C lower temperature mainly in new field of application. Thickness of 5-10 mm of CrN coating shows good adhesion to substrate more corrosion resistant than traditional coating of TiN which are thermally stable up to 700°C.Double TiN + CrN coatings were used as a highly abrasive resistant coating in the production of rotors (in the electromotor industry), and in cold forming and forging in mass manufacturing of screws.

Unal et al. (2004) [12] studied and explored the influence of test speed and load values on the friction and wear behavior of pure polytetrafluoroethylene (PTFE), glass fiber reinforced (GFR) and bronze and carbon (C) filled PTFE polymers. Friction and wear experiments were run under

ambient conditions in a pin on- disc arrangement. Tests were carried out at sliding speed of 0.32, 0.64, 0.96 and 1.28 m/s and under a nominal load of 5, 10, 20 and 30 N. The results showed that, for pure PTFE and its composites used in this investigated, the friction coefficient decrease with the increase in load. The maximum reductions in wear rate and friction coefficient were obtained by reinforced PTFE+17% glass fiber. The wear rate for pure PTFE was in the order of 10-7 mm2/N, while the wear rate values for PTFE composites were in the order of 10-8 and 10-9 mm2/N. Adding glass fiber, bronze and carbon fillers to PTFE were found effective in reducing the wear rate of the PTFE composite. In addition, for the range of load and speeds used in this investigation, the wear rate showed very little sensitivity to test speed and large sensitivity to the applied load, particularly at high load values.

CHAPTER 3

<u>METHODOLOGY</u>

ANSYS (version 14.5) is a finite element program, which is used to do the simulations of the contact problems. There are three different stages namely preprocessing, solution & postprocessing for solving problems. Preprocessing stage involves the preparation of FEM model, element type, real constant, material property & discretization. In Solutions stage ANSYS software automatically generates matrices that describe the behavior of each element, assemble them & computes the unknown values primary field variables such as displacement, temperature etc. In the postprocessing stage results can be analyzed and plotted.

ANSYS is a software application used for both the modeling and analysis of mechanical components and assemblies (pre-processing) and visualizing the finite element analysis result. It is a general-purpose Finite-Element analyzer that employs implicit integration scheme. This runs as a background process and does the real numerical calculations. After completion of simulation, the results can be monitored in the post processing phase. ANSYS is also used to view, plot and process the data. Geometry is made in design modeler of workbench platform itself and then meshing is done in model section.

3.1 The design modeler

There are several ways to make or load parts into the part module. In ANSYS there is a drawing feature, which makes it possible to draw the parts. Because the shapes of the parts are very easy to draw, this feature is used. Modeling is done in millimeters, so the other quantities have to be of the same order.

3.1.1 Modeling the pin

The real pin design is shown in figure 3.1. The pin and clamp holder can be modeled exactly in the ANSYS workbench but creates a difficulty in strange structured elements (in case of the used octahedral elements, see section mesh). Again the CPU-time will be too large. It is better to only model the part of the pin that is extending the clamp and make proper boundary conditions for the top surface. The pin is extending about 15 millimeters. When a connection is made between the models, the contact surface area dimensions are the same, with similar contact behavior and probably pressure distribution. In this way it is easier to compare the two models. First an

intersection of the pin is drawn at the position in the co-ordinate system, where it is situated the assembly. Then only one translation is needed to get the pin at its right position. The dimensions of the pin used in the FE-analysis are shown in table 3.1. In table 3.2, the properties of this part are shown.
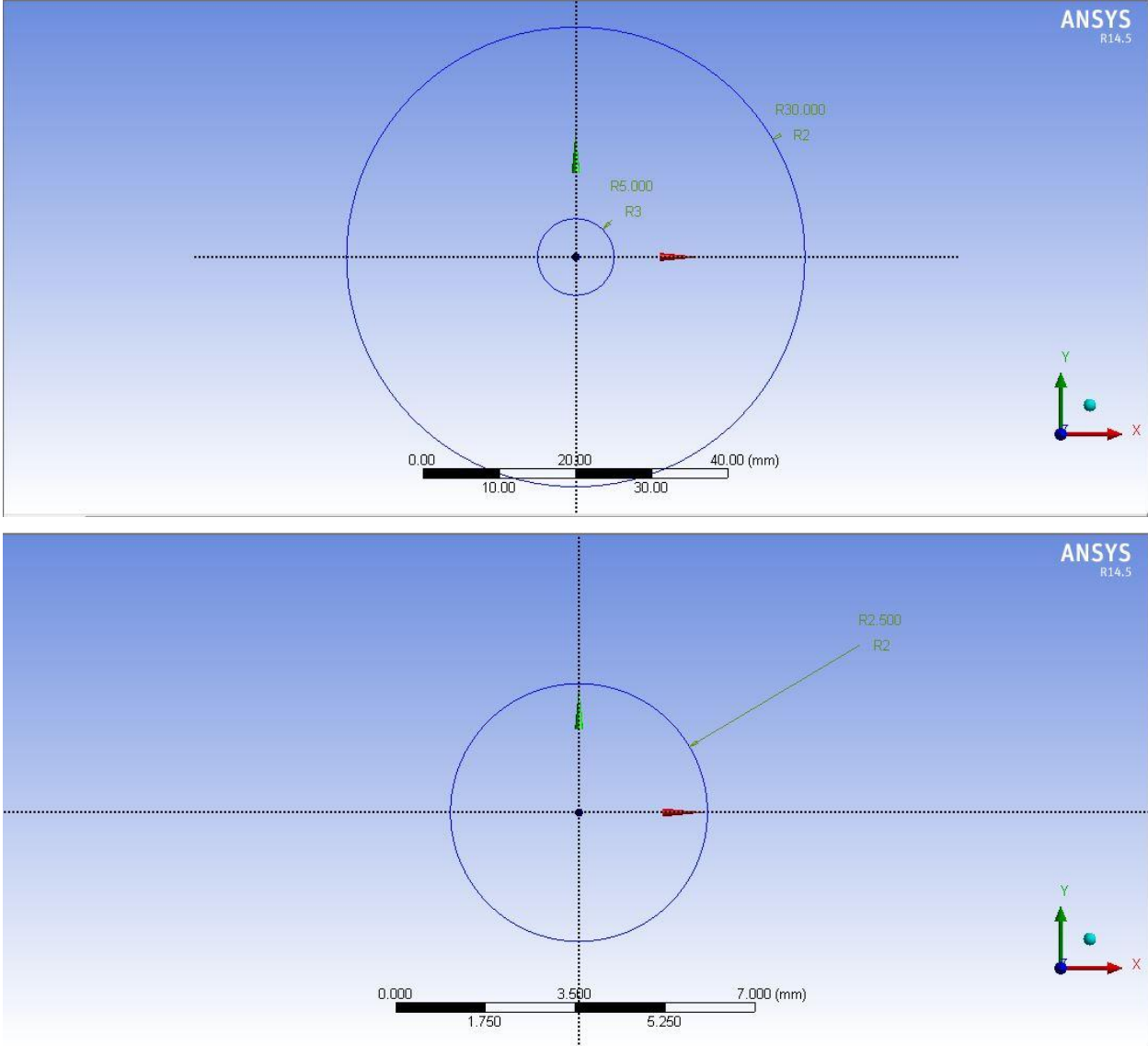

Figure 3.1: Pin and disc dimensions

Table 3.1: Dimensions of the pin and disc in the ANSYS-model.

The Disc		The Pin	
Outer radius	30 mm	radius	2.5 mm
Inner radius	5 mm	Thickness (depth)	15 mm
Thickness (height)	5 mm		

Figure 3.3 is also used to determine the dimensions of the disc. At the center a hole is made for the same reasons. The center of the pin acts at a radius of 20 [mm] at the disc. This is exactly the middle between the inside and outside radius of the disc. The track on which the pin can run is 5 millimeters wide. The dimensions of the pin and the disc used for the ANSYS-model are presented in table 3.1. The settings for the disc are presented in table 3.2.

Table 3.2: Part properties.

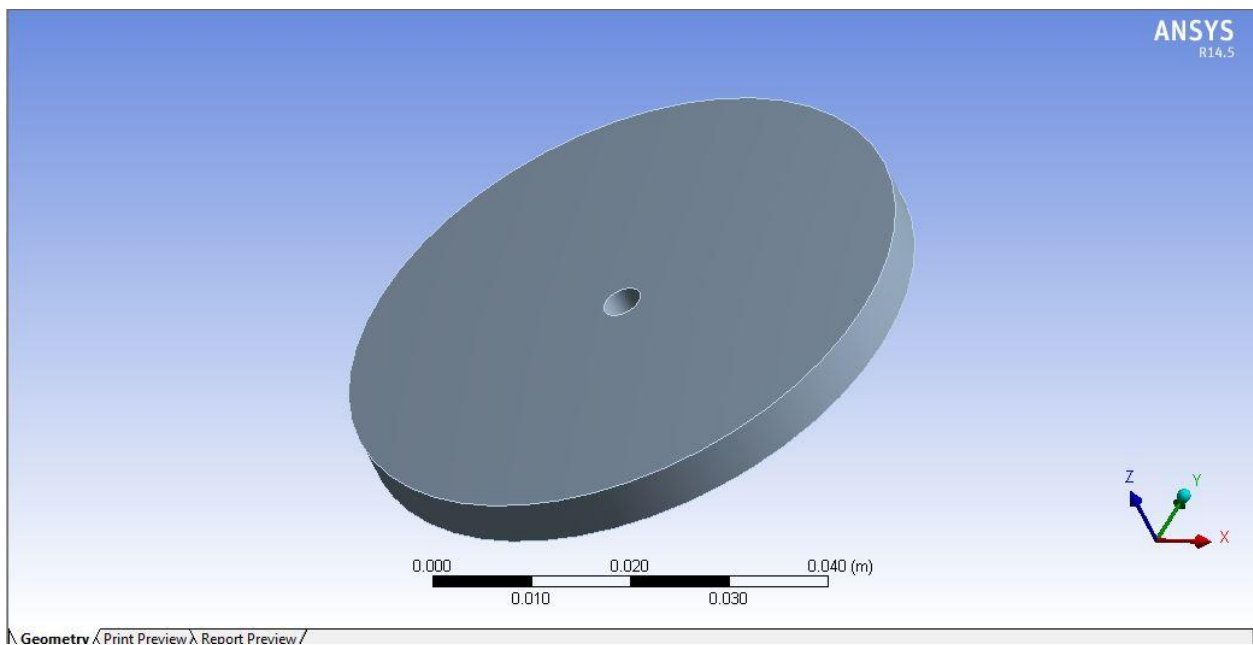| Part Name	Modeling space	Type	Base feature	
			Shape	Type
Pin	3D	Deformable	Solid	Extrusion
Disc	3D	Deformable	Solid	Extrusion
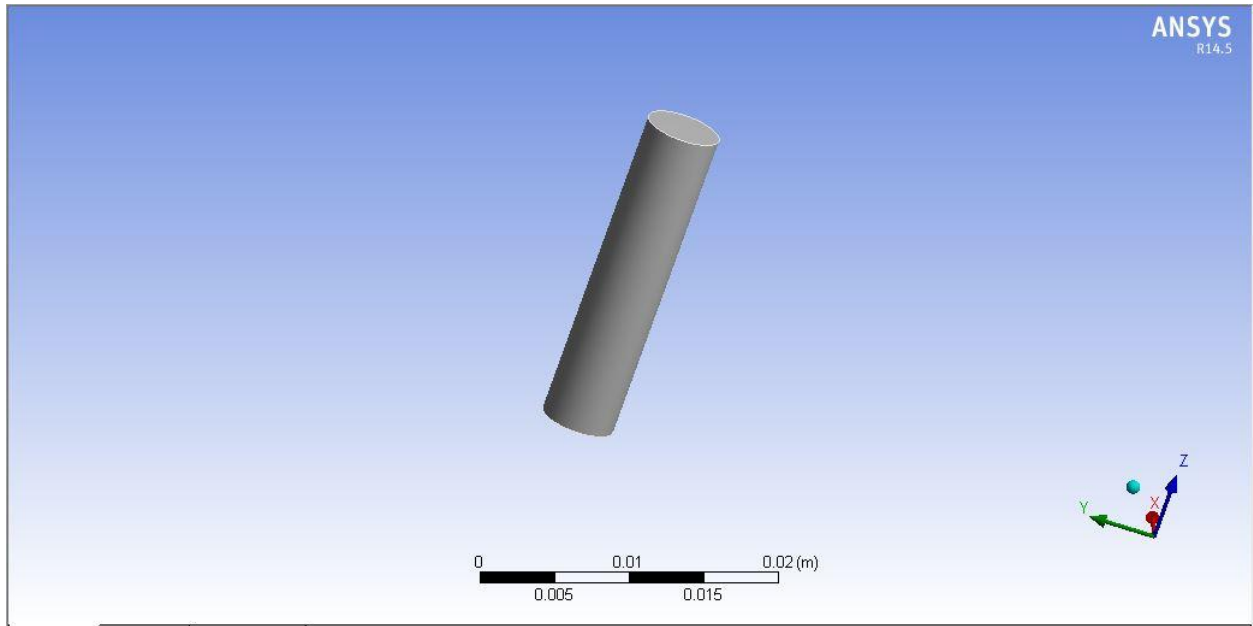
Figure 3.2: The test disc and pin in ANSYS.

The simualtion is further processed in ANSYS 14.5 in the model menu of workbench and loads and boundary conditioned is specified there as shown in figure 3.3.But due the unappropreiate boundary condition or contact defination the analysis is not able to solve the equation generated in the earlier steps because of the Multi point contact error.

Figure 3.3 Loads and boundary condition in ANSYS.

For the solution of model the further analysis is done on ABAQUS 6.13, and geometry is imported in the part module of ABAQUS CAE. Figure 3.5 shows the flow chart of steps used in ABAQUS .

Figure 3.4 :ABAQUS software product's order of use.

```
┌─────────────────────┐
│  Import Pin and Disc in │
│     Part Module      │
└─────────────────────┘
           │
           ▼
┌─────────────────────┐
│  Specify property and │
│   Assign Section in   │
│    Section Module     │
└─────────────────────┘
           │
           ▼
┌─────────────────────┐
│ Assemble the Disc and Pin │
│   in Assembly Module  │
└─────────────────────┘
           │
           ▼
┌─────────────────────┐
│   Define two separate │
│   steps in Step Module │
└─────────────────────┘
           │
           ▼
┌───────────────────────────┐
│ Define friction interaction between │
│  pin and disc in Interaction Module │
└───────────────────────────┘
           │
           ▼
┌─────────────────────┐
│   Apply load and BCs  │
│     in Load Module    │
└─────────────────────┘
           │
           ▼
┌─────────────────────┐
│    Mesh pin and disc  │
│    in Mesh Module     │
└─────────────────────┘
           │
           ▼
┌─────────────────────┐
│   Assign job in Job   │
│       Module          │
└─────────────────────┘
           │
           ▼
┌─────────────────────┐
│    See results in     │
│    Visualization      │
│       Module          │
└─────────────────────┘
```
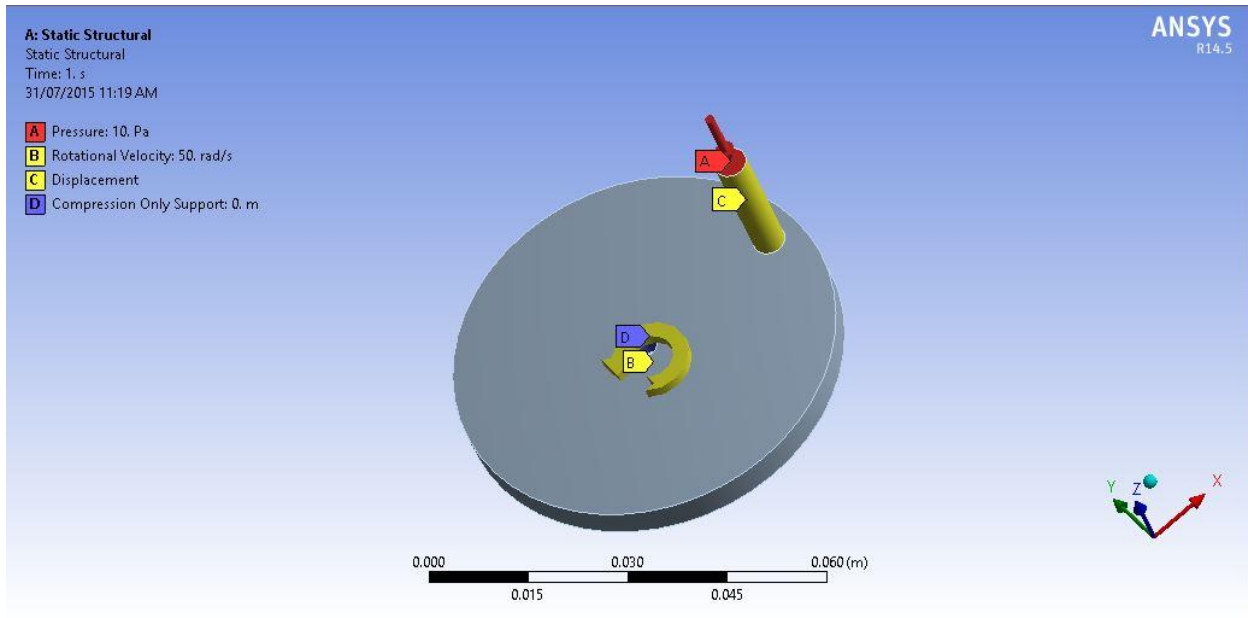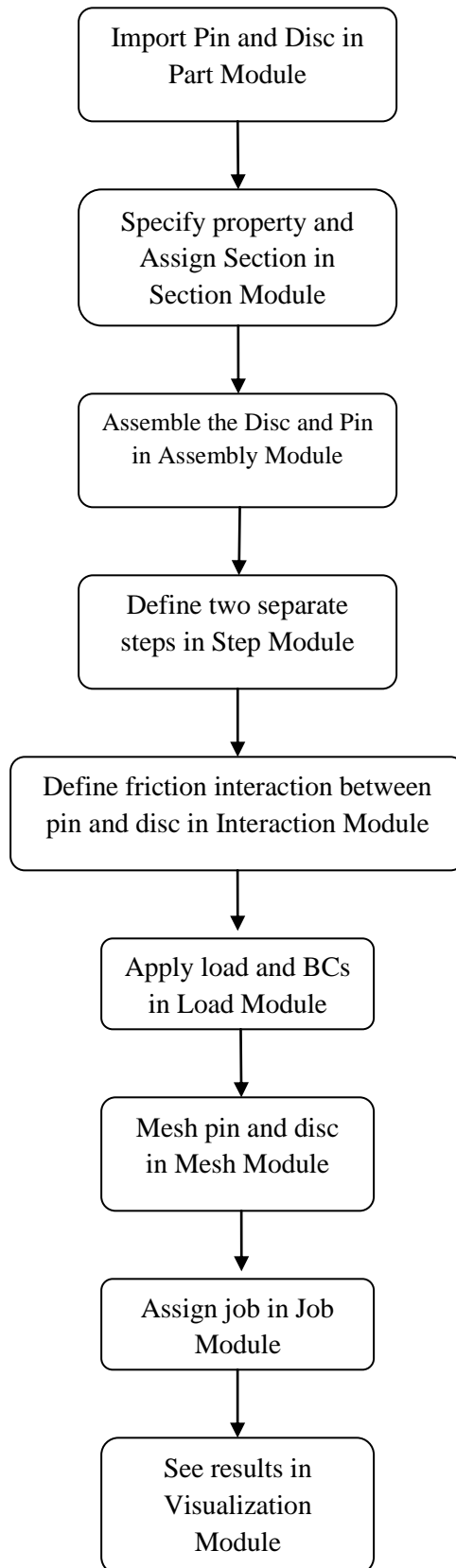
Figure 3.5: Flow chart of steps used in ABAQUS.

[27]

3.2 Property module

In the property module the material properties of chard chrome (Disc) and cylinder liner (Pin) are specified and body sections are assigned to specified regions of the pin and the disc. The disc and pin consists of one material and one section. In table 3.3 the different material properties are presented.

Table 3.3: Material properties.

Section Name	Material Behavior	Type	Young's Modulus [N/mm2]	Poisson's Ratio	Section Type
Pin	Mechanical, Elastic	Isotropic	150000	0.3	Solid/Homogenous
Disc	Mechanical, Elastic	Isotropic	103420	0.29	Solid/Homogenous

3.3 Assembly module

A new co-ordinate system is created in this part. The pin and disc are loaded and assigned under this co-ordinate system. First the disc part is loaded and positioned at the center of the co-ordinate system. Then, pin is loaded and by using the translation command, it is placed at (22,0,5). In this way it is located at 22 mm from centre on the top surface of disc. The top surface of pin and disc are constrained to be parallel.

In the assembly module, it is also possible to create sets of lines, nodes and surfaces. These are useful to make it easier to select lines, nodes and surfaces during refining mesh. If number of objects are more then it will be very difficult to select them separately each time. With really fine meshes, it is almost impossible to select every single object.
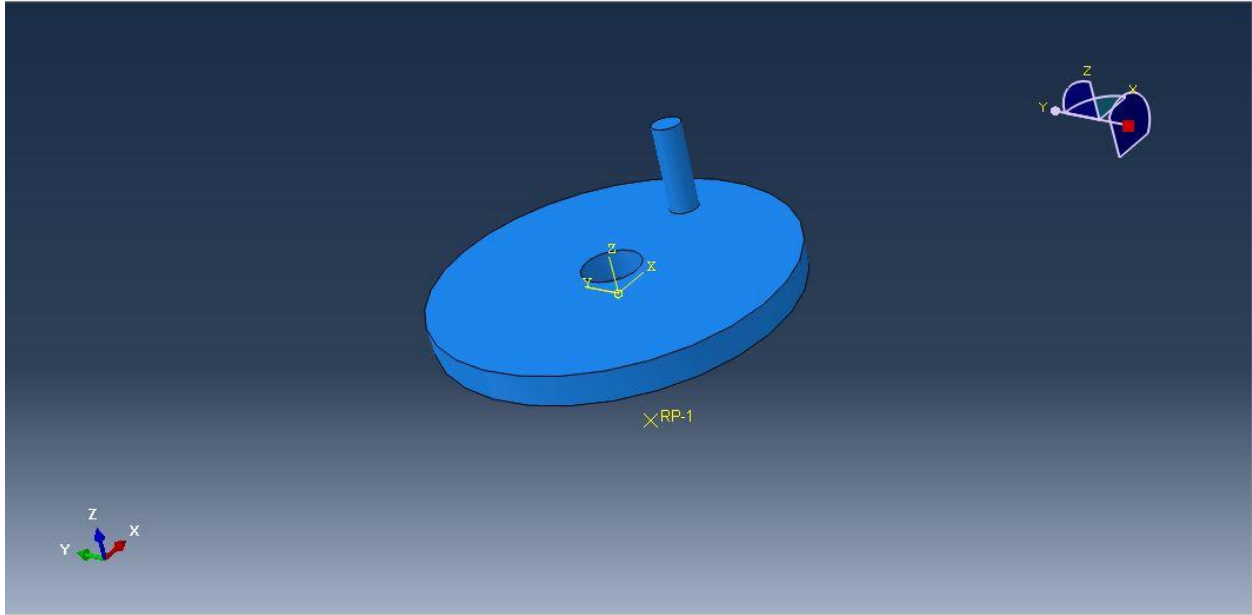
Figure 3.6: Assembly of pin and disc

3.4 Step module

The step module is used to create different steps for analyzing. It is useful to make a single step for each change in the model. In every step can be prescribed what the output parameters have to be. Also the length of the step, the actual simulation time, can be set. As well as the start, minimum and maximum value of a single increment and the maximum number of increments.

In the initial step the model is checked or it is modeled in a correct way. In the first step the force is applied at the top surface of the pin. A ramp function is used to apply the force. In the second step this force is maintained and the disc starts to rotate with a prescribed speed. The length of this step determines the length of the path at the disc. The settings are presented in table 3.4.

Table 3.4: Step properties.

Step	Step name	Procedure	Time [s]	Maximum number of increments	Increment size		
					Initial	Min.	Max.
0	Initial	Initial	N/A	N/A	N/A	N/A	N/A
1	Apply Pin Force	Static, General	1	10	0.1	0.1	1
2	Rotate Disc	Static, General	5	100	0.1	0.001	1

3.5 Interaction module

3.5.1 Interaction of the surfaces

In order to let the model run well a friction formulation is prescribed for the contact between the pin and the disc surfaces. There are a few models to prescribe the friction between the pin and disc. In the first model a penalty of 0.15 will prescribe the friction, because this is the average CoF out of the results of the PoD-tests. In table 3.5 the initial friction conditions are given.

Table 3.5: Interaction properties.

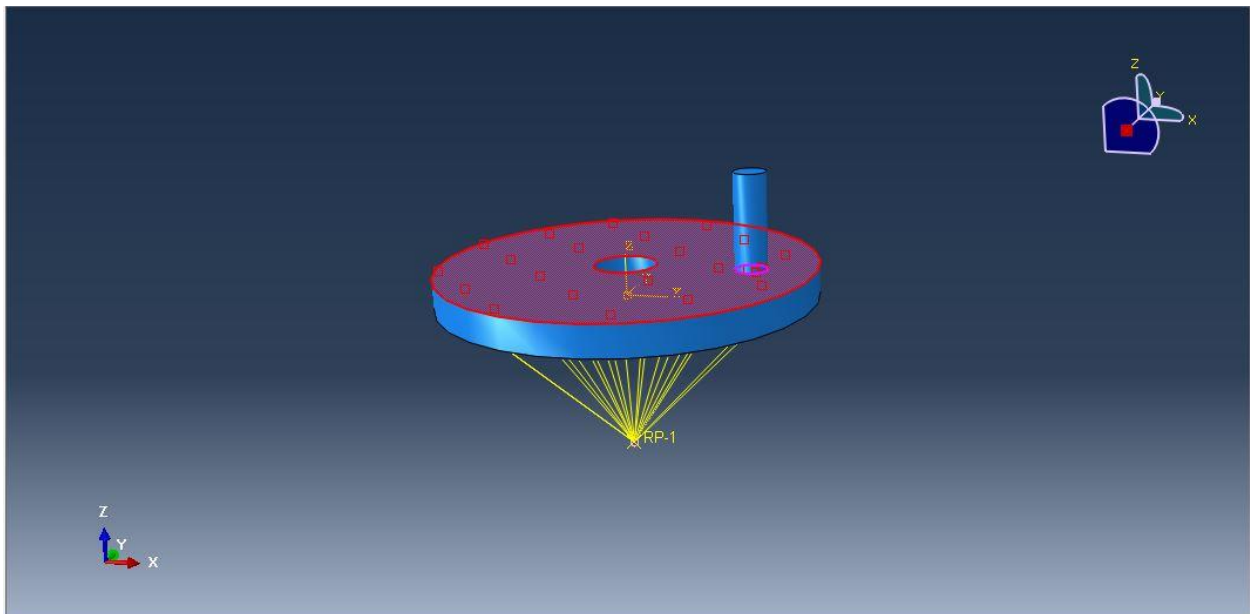| Interaction	Contact property	Friction formulation	CoF
Pin surface/disc surface	Tangential behavior	Penalty	0.3

Figure 3.7: Interaction between Pin and Disc.

3.5.2 Disc rotation

In order to be able to control the movements of the disc a coupling has to be prescribed. With the RP assigned in the part module, it is possible to control the disc by one single point, see table 3.6. The RP is set as the control point and the bottom surface of the disc is the controlled region. The complete surface is selected because when only the outer region is selected the results will

be influenced by the bending of the disc, which is neglected because it is not appearing. Now every single point on the surface has the same boundary conditions (BC's) instead of only the outer region. A kinematic coupling is chosen instead of a distributing coupling. In case of a kinematic coupling all the DOF (Degrees Of Freedom) at the coupling nodes are eliminated and the coupling nodes will be constrained to move with the rigid body motion of the reference node. In case of a distributing coupling, the DOF are not eliminated, but are enforced in an average sense. This means that the resulting forces at the coupling nodes are equivalent to the forces and moments at the reference node.

Table 3.6: Constraint properties.

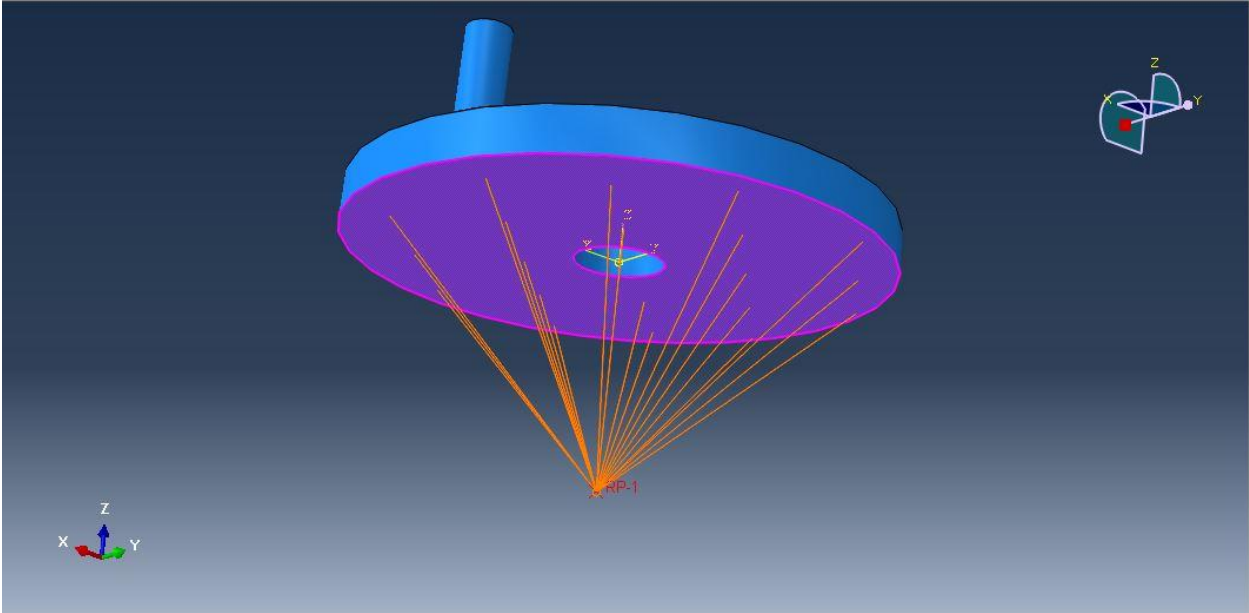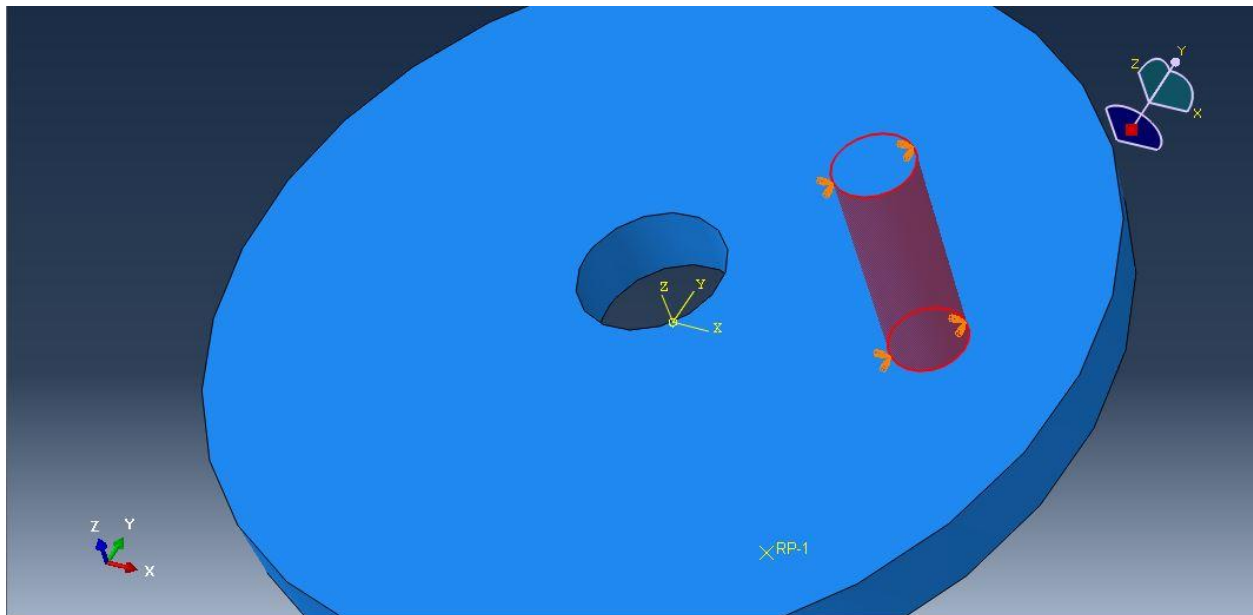| Constraint	Constraint type
Disc / RP	Coupling

Figure 3.8: Coupling.

3.6 Load module

3.6.1 Boundary conditions

To simulate the clamping of the clamp holder it is important that the BC' s (Boundary Condition) are chosen in a proper way. The BC's should not generate extra stresses in the pin and it should be able to apply a force on the top. Using a coupling for the disc is not possible because the material will not able to move after this due to its poison ratio. Therefore, the outer surface of pin is fixed in x and y direction whereas the movement is free in z direction. All these BC's on the surface make sure that the surface is able to move towards the disc in the z direction and that the surfaces of the pin and disc stay aligned. The BC's make it also possible that the material can act to its poison ratio. So the material is able to deform. See figure 3.8 and table 3.7 for the boundary condition on pin and disc.
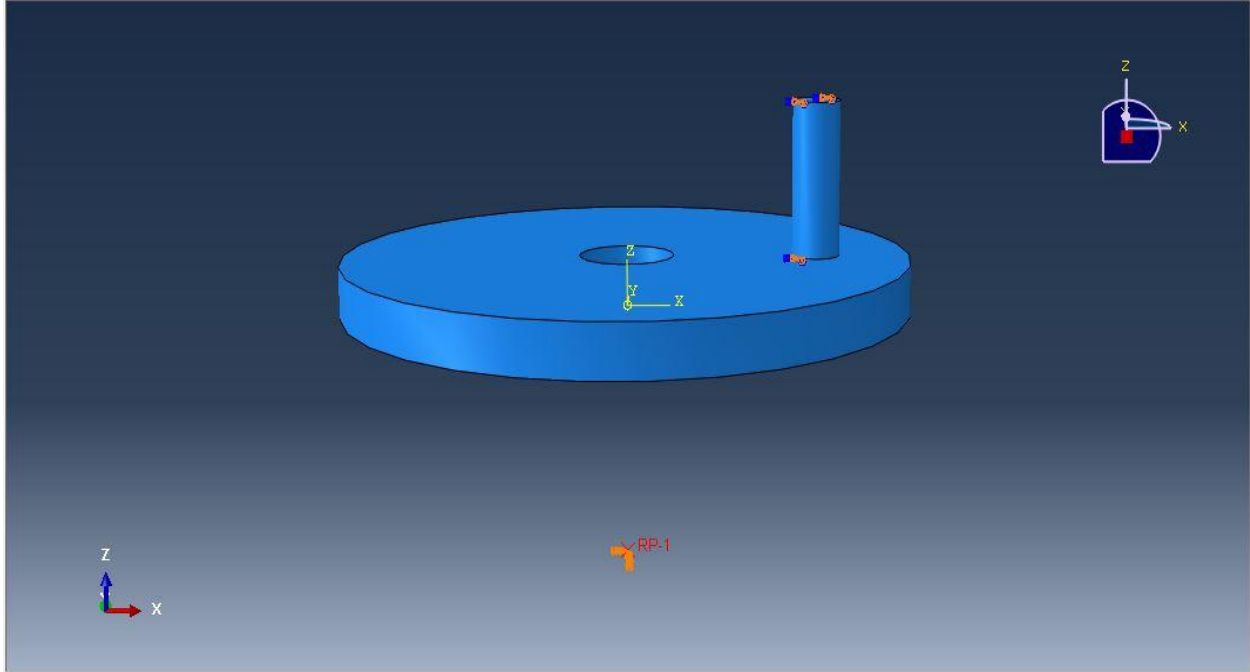
Figure 3.9: The boundary conditions of the pin and the disc.

The previous prescribed constraint of the disc is used in the load module. Angular velocity is prescribed for the RP around the z-direction axis. The other movements, rotations and translation are suppressed. This should be done because there is no backlash at the disc shaft and in the clamp holder part as well.

3.6.2 Load

There are two ways in which a force can be prescribed on the top surface. The first one is to make a force vector to act at a node. The second option is two let a pressure act on a surface. The second one is the best. The first option results in a non homogenous force distribution in the upper part of the pin. When a pressure is applied at the top surface the size of the surface is of no importance because the quantity is prescribed in force per unit area and the pressure is distributed equally over the complete top surface. The values of pressure at different load have been calculated using equation 3.1 and are given in table 3.8. The applied pressure is only acting on the highest surface in the figure to keep the figure clear. In the first step of applying the pressure it can be seen that the pressure distribution is done in the right way, because the von mises stresses at the top surface have all the same color. This means that the stresses have the same value.

$$Pr = \frac{P}{A} \tag{3.1}$$

Table 3.7: Load condition.

Load condition	Direction	Step 1	Step 2
Pressure at top pin surface	perpendicular to surface	VALUE*	Propagated

Table 3.8: Pressure values.

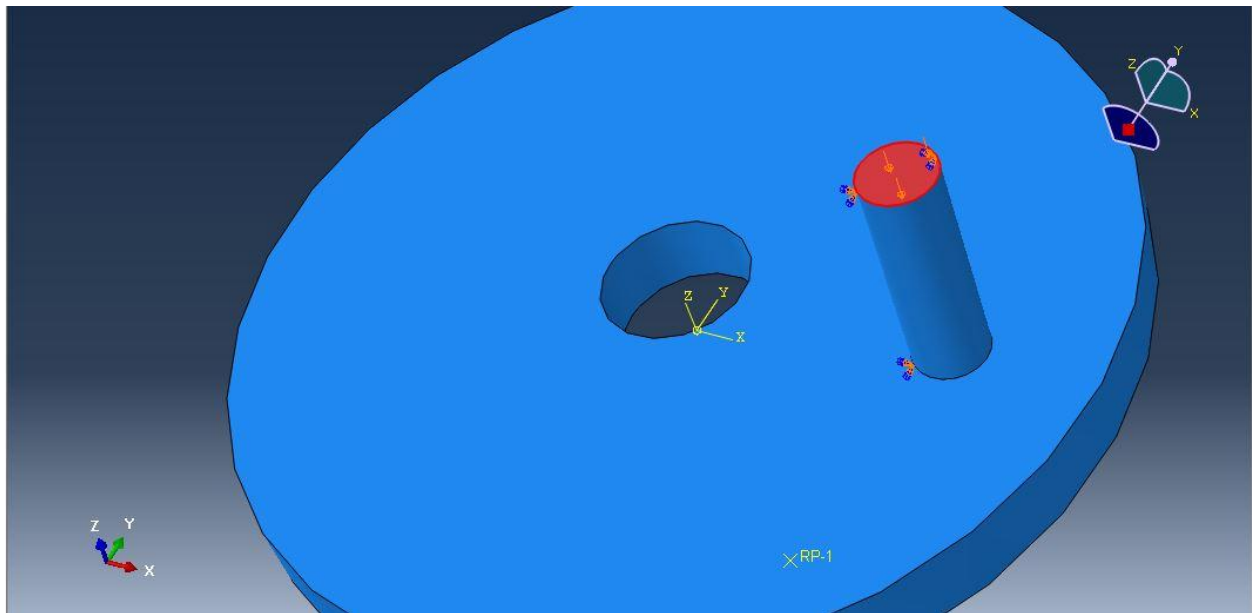| Load (N)	Pressure (MPa)
50	2.564
60	3.055
70	3.565
80	4.074
90	4.583
100	5.093

Figure 3.10: Load.

3.7 Mesh module

As already mentioned the used elements are of the type C3D8, see table 3.9. It is a continuum solid element. It has 8 nodes, at each corner 1. This is the best option, since the model is made in such a way that the elements are almost square in the contact region. This is needed in order to

get good results. The element must be able to "feel" what is happening at the other side of the element. When the brick is long and narrow, this is not possible, and the obtained results will be not very reliable. Another option is the C3D6-element. This is a 6-nodes linear triangular prism. Verhoeven [1] has already researched this option and came to the conclusion that the C3D8-elements were the best option to do analyses with. Because for further research the outcome of this research is going to be implemented in Verhoeven's model, it is useful to use the same kind of elements. The comparison is easier when elements are kept of the same type. To get the desired amount of elements on each edge the seed edge feature is used. The edges are selected as sets edges with the same amount of desired elements on each edge.

In order to reduce the number of elements, other three sections of the disc should contain less number of elements since they have no physical contact with the pin. Therefore, it is possible to apply a lower number of elements. Because all the nodes of the each element have to be connected to each other, the number of elements in the radial and height direction they have the same value (resp. 7 and 4). The number of elements in the tangential direction has a lower value, 9 elements. These elements have a long cuboid form.
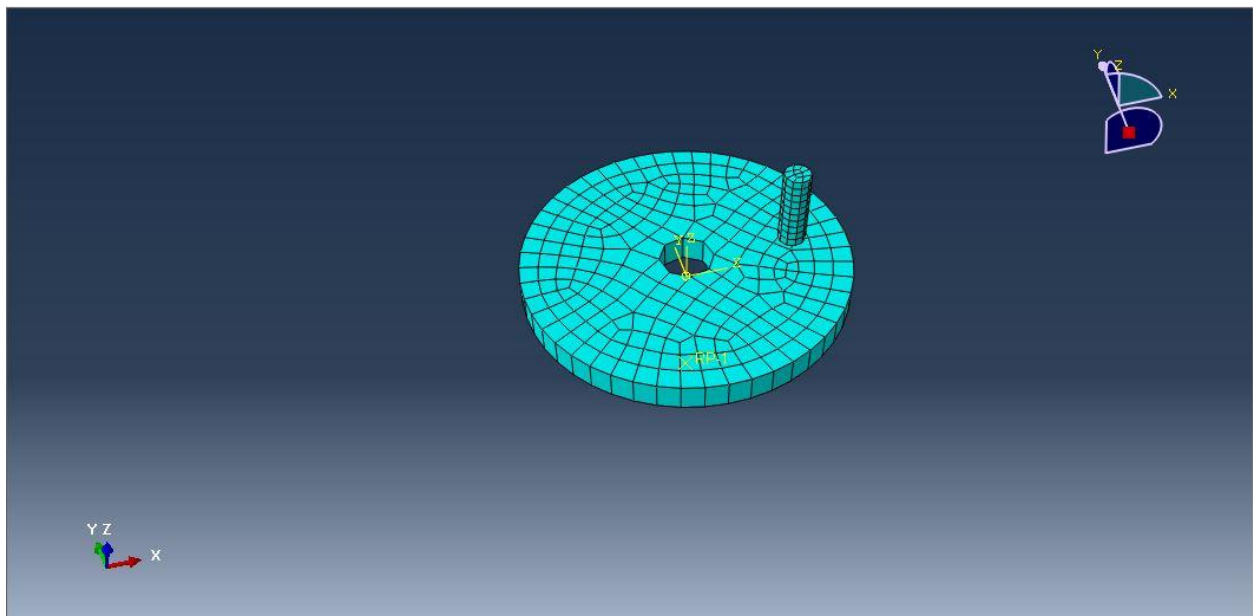

Figure 3.11: Mesh

Table 3.9: Mesh properties.

Part name	Element type	Element type description
Disc	C3D8	8-node linear brick
Pin	C3D8	8-node linear brick

3.8 Job module

After finishing the physical modeling, the job can be submitted for analysis. The program will checked if all settings are correct and it will also be checked for the availability of requested output variables. The first jobs run on a computer with a small processor, so the memory the program is allowed to use is set on 256 Mb. Even though it is not a complicated large model so it runs fast. During running of job, the progress of analysis can be checked by the monitor function. The settings for this module are shown in table 3.10.

Table 3.10: Job manager.

Job name	Model	Type	Run mode
PoD_job_001	Model-1	Full analysis	Background

CHAPTER 4

RESULTS AND DISCUSSIONS

In the visualization module the parameters have to be selected for the results. Looking at the animation of the simulation makes clear that the boundary conditions of the pin are chosen properly. There are no extra stresses generated around the boundary conditions at the top pin. Stresses due to the BC's could be clearly seen. When a plot is made of the nodes at the lower surface of the disc part of the z-direction, no meaningful displacement occurs (order 1.10^{-15} in the contact area). This means that the BC of the disc is chosen in the right way as well.

In the first step the pressure is nicely equally distributed, because the model has one color at each increment, the von Mises stresses are of the same magnitude in every point in the pin. This is what is desired. A top view of the disc shows that there is symmetric spot of stresses in the disc around the pin. That it is completely round is due to round form of the pin. An intersection of the disc shows that the thickness of the disc is chosen properly. Large stresses occur only in the upper part of the disc.

Also in the second step can be seen that at the inside of the pin (near the disc center) the stresses are higher than at the outside of the pin. When the disc rotates and the normal force is pushing at the top of pin, the pin tends to stick, together with the movement it causes a little bending of the pin. The front of the pin is pushed into the disc and at the back it lifts up a little according to the front. Because the circular movement of the disc the stresses at the inside of the pin are higher then at the outside of the pin.

The disc stresses in the second step are floating a little bit. Again due to the rough mesh. The stresses at the front of the pin are higher than at the end of the pin. And the stresses near the center of the pin are higher than at the outer radius. According to what has been explained for the pin this is according to each other.

To make sure that the model is correct the different values of the quantities have to be checked. The values that will be checked are summarized below. An approach of what the values should be, are calculated with the equations presented in chapter 1. The prescribed values should have a certain value at a certain point in the simulation.

1. The contact pressure in the last increment of the first step should be equal to the applied pressure.

2. The magnitude of the reaction forces should be around $F_{CoF} = N.\mu$

3. The rotational displacement of the nodes should be equally to what is prescribed, $\omega = 2\pi N/60$ [s].

Table 4.1: Angular velocities.

N (rpm)	ω (rad/s)
50	5.236
60	6.283
70	7.33

4.1 Contact pressure

The values of contact pressure are obtained in visualization model under CPRESS drop down menu. The value of contact pressure is recorded for the every step to get the wear depth. It can be seen that the magnitude of contact pressure is increasing by increasing the load at the constant speed.

Table 4.4: Contact pressure at 70 rpm.

S. No.	Load(N)	Contact Pressure(MPa)
01	50	4.162
02	60	4.912
03	70	5.732
04	80	6.55
05	90	7.369
06	100	8.169

Table 4.3: Contact pressure at 60 rpm.

S. No.	Load(N)	Contact Pressure(MPa)
01	50	3.588
02	60	4.279
03	70	4.993
04	80	5.699
05	90	6.415
06	100	7.128

Table 4.4: Contact Pressure at 70 rpm.

S. No.	Load(N)	Contact Pressure(MPa)
01	50	4.247
02	60	5.056
03	70	5.906
04	80	6.747
05	90	7.597
06	100	8.433
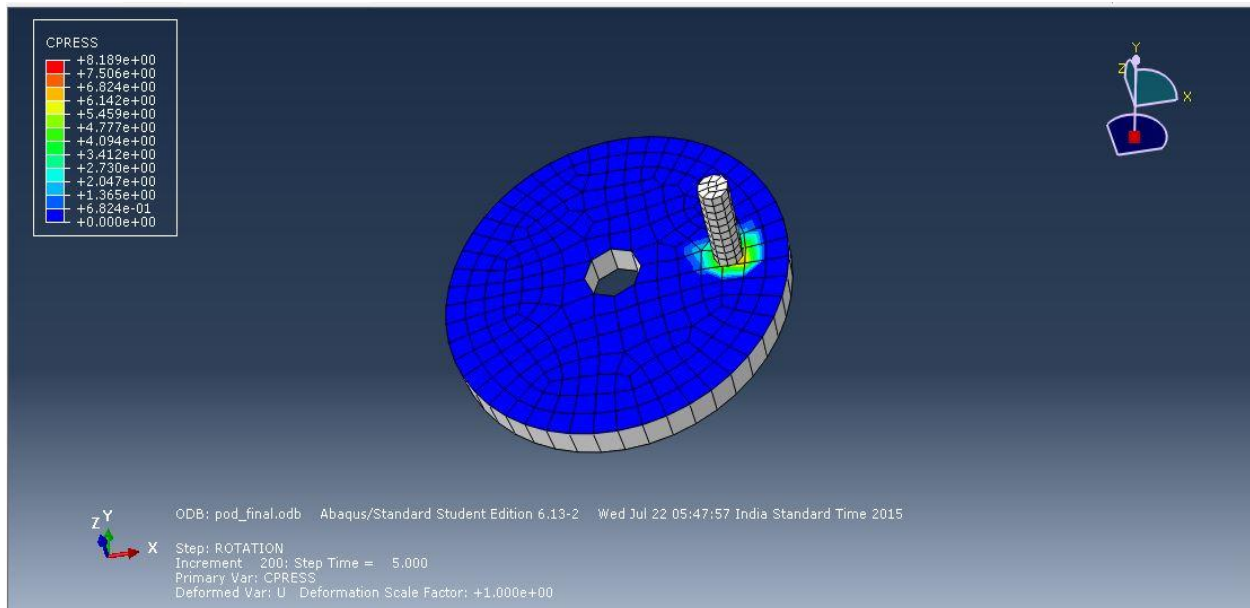
Figure 4.1: Figure representing Contact pressure.

4.2 Displacement

The displacement of the pin is also known. Because it is of a round feature, the mean displacement of center of pin on the disc is calculated. The displacement is calculated with 4.1.

$$d = r.t.v \qquad\qquad (4.1)$$

Where,

r= distance of center of pin from the center of disc.

t= simulation time.

v= sliding velocity of disc.

Since pin is located at 20 mm from the center of pin hence r=20 mm and in the step module we specified the simulation time as 5 second hence t=5 second. The table 4.5 shows the values of displacement at different rpm considered in this project.

Table 4.5: Displacement of pin.

S. No.	Angular velocity ω	Displacement (mm)
01	50	523.6
02	60	628.3
03	70	733.03

4.3 Specific wear rate

The value of specific wear rate K is taken constant by assuming that it is not varying for the same material under changing load condition .The K value used in this project work is taken from earlier research work done on hard chrome disc and cylinder liner pin experimental setup in pin on disc test. I have taken the mean value of specific wear rate K i.e. 6.10^{-05}.

4.4 Wear Depth

As earlier mentioned in the introduction part of the thesis, the equation we are using for the calculation of the wear depth is most popularly accepted Archard equation. The key outcome expected from an FEA wear analysis is contact pressure (CPRESS). The contact pressure magnitude is recorded for all the sets of inputs. And specific wear rate value is taken from the experimental analysis and sliding distance is calculated from the input parameters. And finally

by putting all the values in archard equation the wear depth is calculated for all sets of inputs. Table 4.6a, 4.6b,4.6c shows the calculated wear depth for 50 , 60 ,70 rpm respectively .

Table 4.6 a: Wear at 50 rpm

S. No.	Load(N)	Wear (μm)
01	50	0.1307
02	60	0.1543
03	70	0.18
04	80	0.20577
05	90	0.2315
06	100	0.25726
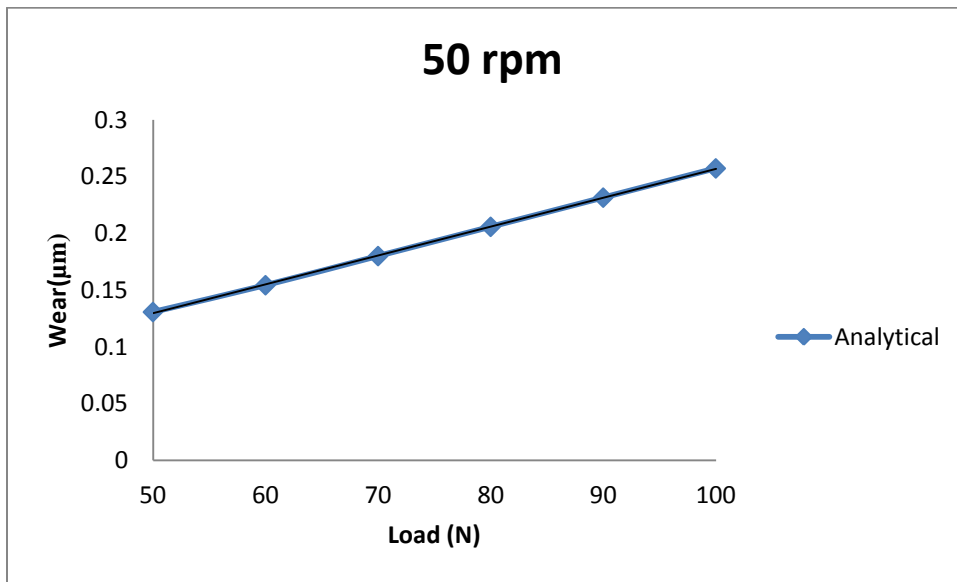
Figure 4.2: Wear versus load graph at 50 rpm.

Table 4.6b: Wear at 60 rpm

S. No.	Load(N)	Wear (μm)
01	50	0.13526
02	60	0.1613
03	70	0.18822
04	80	0.21484
05	90	0.24183
06	100	0.2687
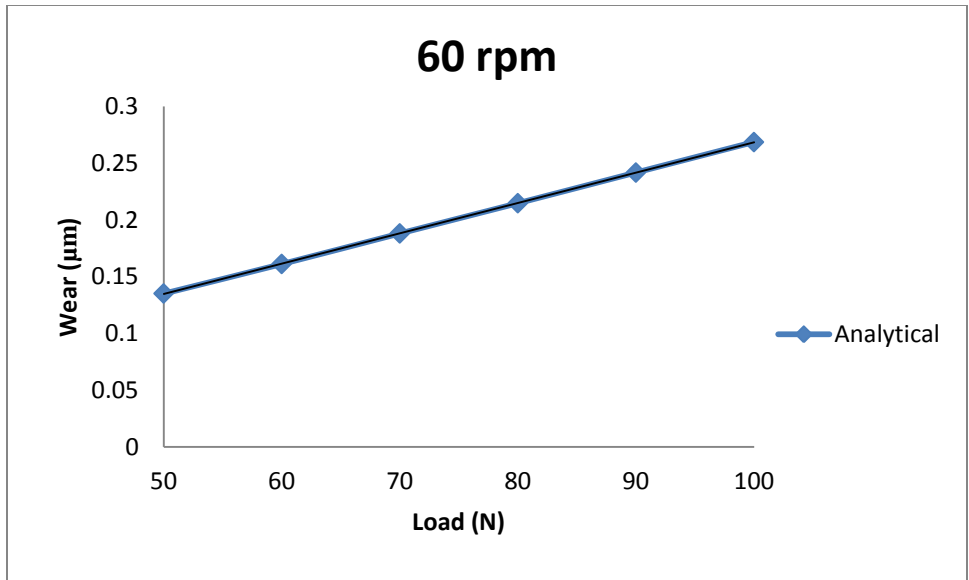
Figure 4.3: Wear versus load graph at 60 rpm.

Table 4.6c: Wear at 70 rpm.

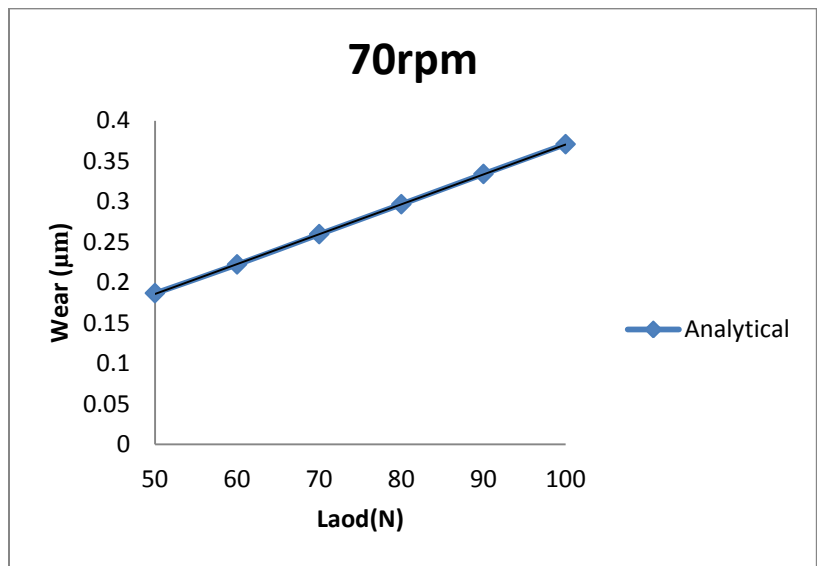| S. No.	Load(N)	Wear (µm)
01	50	0.18686
02	60	0.22237
03	70	0.25975
04	80	0.29674
05	90	0.3341
06	100	0.3709

Figure 4.4: Wear versus load graph at 70 rpm.

As we can interpret from the above graphs that the wear depth goes on increasing with the increase of load at constant speed as well as the angular velocity.

4.5 Experimental validation

For any simulation work validation is most important to verify the accuracy of the simulation work. For the experiment purpose hard chrome disc and cylinder liner pin is tested in pin on disc apparatus with same parameters as used in simulation work i.e. sliding speed, load and running time. Then the values of wear depth have been noted down and mentioned in table 4.7 a, 4.7 b, 4.7 c.

Table 4.7 a: Experimental values of wear at 50 rpm.

S. No.	Load(N)	Wear (µm)
01	50	0.1286
02	60	0.1524
03	70	0.18232
04	80	0.21478
05	90	0.2426
06	100	0.26289

Table 4.7 b: Experimental values of wear at 60 rpm.

S. No.	Load(N)	Wear (µm)
01	50	0.1432
02	60	0.18711
03	70	0.20351
04	80	0.22841
05	90	0.2517
06	100	0.28459

Table 4.7 c: Experimental values of wear at 70 rpm.

S. No.	Load(N)	Wear (µm)
01	50	0.18422
02	60	0.23245
03	70	0.26241
04	80	0.3113
05	90	0.3569
06	100	0.39287

To compare the results of simulation and experiment graphically, graph is drawn in MS excel. The experimental results and simulation results are almost similar, it means the performed simulation work is done in the right way. Figure 4.5,4.6 4.7, shows the comparative graph between analytical results and experimental results.
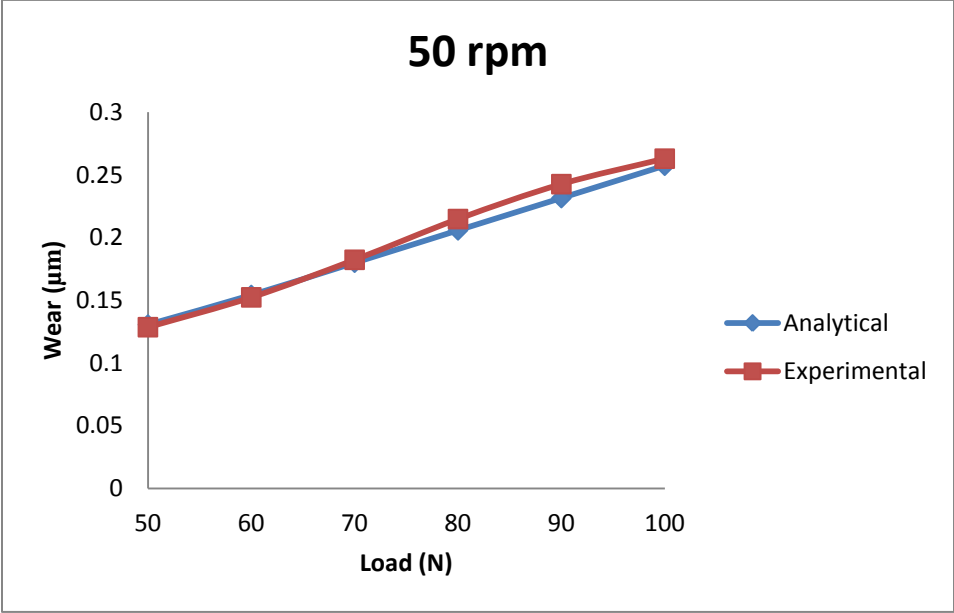

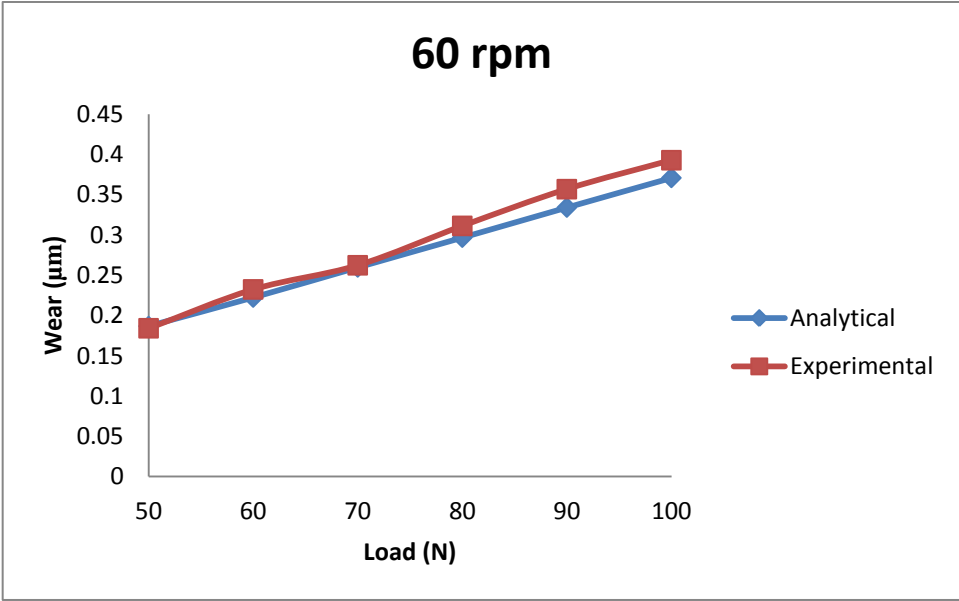Figure 4.5: Comparative wear versus load graph at 50 rpm.

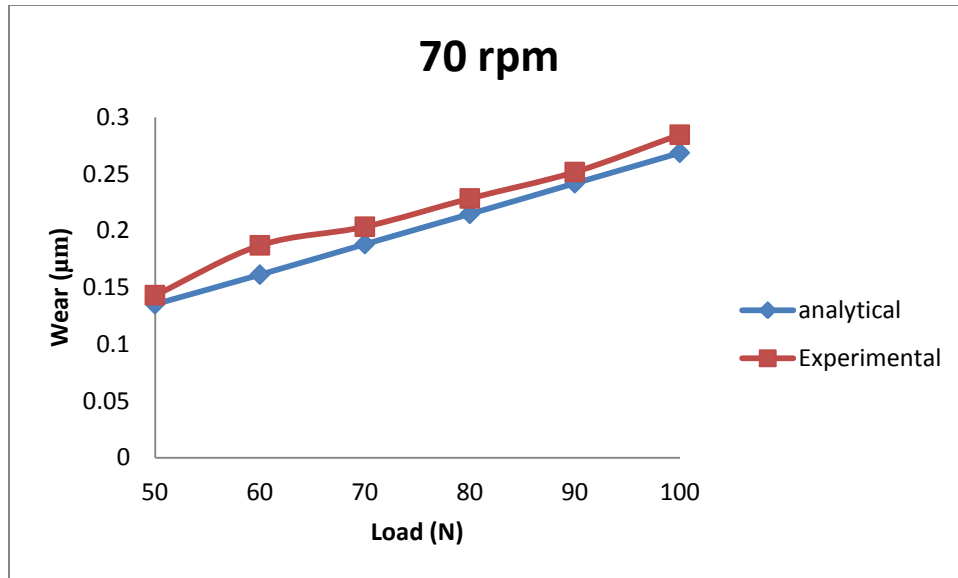Figure 4.6: Comparative wear versus load graph at 60 rpm.

Figure 4.7: Comparative wear versus load graph at 70 rpm.

From the above figures and result we can conclude that contact analysis in ABAQUS and experimentally pin on disc both of them, similar results are found which shows increase in load and angular velocity wear depth also increases. The two important outcomes expected from a wear model from engineering standpoint are: change in dimensions and localized effects of wear. The FEA model presented addresses both aspects. Dimensional changes resulting from wear are seldom uniformly distributed; therefore any wear prediction model averages the changes in dimension across the contact in consideration. The FEA model can gives wear results at nodal level which can be averaged across the contact.

4.6 Effect of pin diameter

It is generally assumed that the wear rates increases as the contact area is increased. This hypothesis was investigated in this model, with pin diameter ranging from 5-8 mm, giving nominal contact pressures from 4.162-1.48 MPa. And since the wear depth is directly proportional to the contact pressure, it means wear depth will decreases with increasing contact area. Table 4.8 indicates the contact pressures with change in diameter. The earlier experiment suggest that the milder wear processes with the larger diameters, while the smaller diameters

exhibited transverse ripples and cracks and detachment of thin layers from the surface. The percentages of granules (mostly submicron), fibrils and flakes, and the sizes of these particle types were similar among all pin diameters. This work supports the hypothesis that larger contact areas, up to the maximum area tested in our study, produce lower wear rates.

Table 4.8: Contact pressure for different diameter of pin.

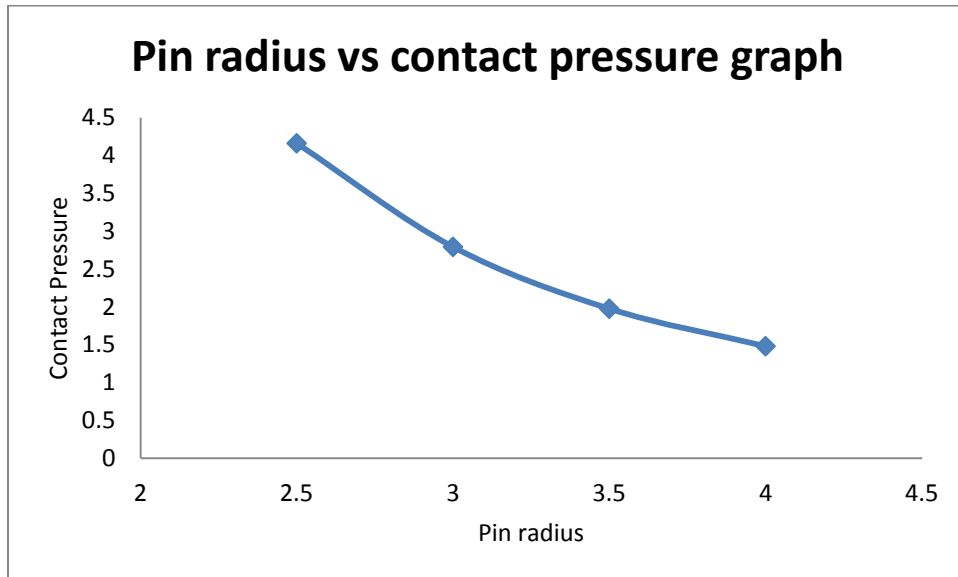| S. No.	Pin radius (mm)	Pin area (mm^2)	Load applied (N)	Pressure on pin top surface (MPa)	Contact pressure (MPa)
01	2.5	19.16	50	2.564	4.247
02	3	28.274	50	1.768	2.793
03	3.5	38.484	50	1.3	1.976
04	4	50	50	1	1.48

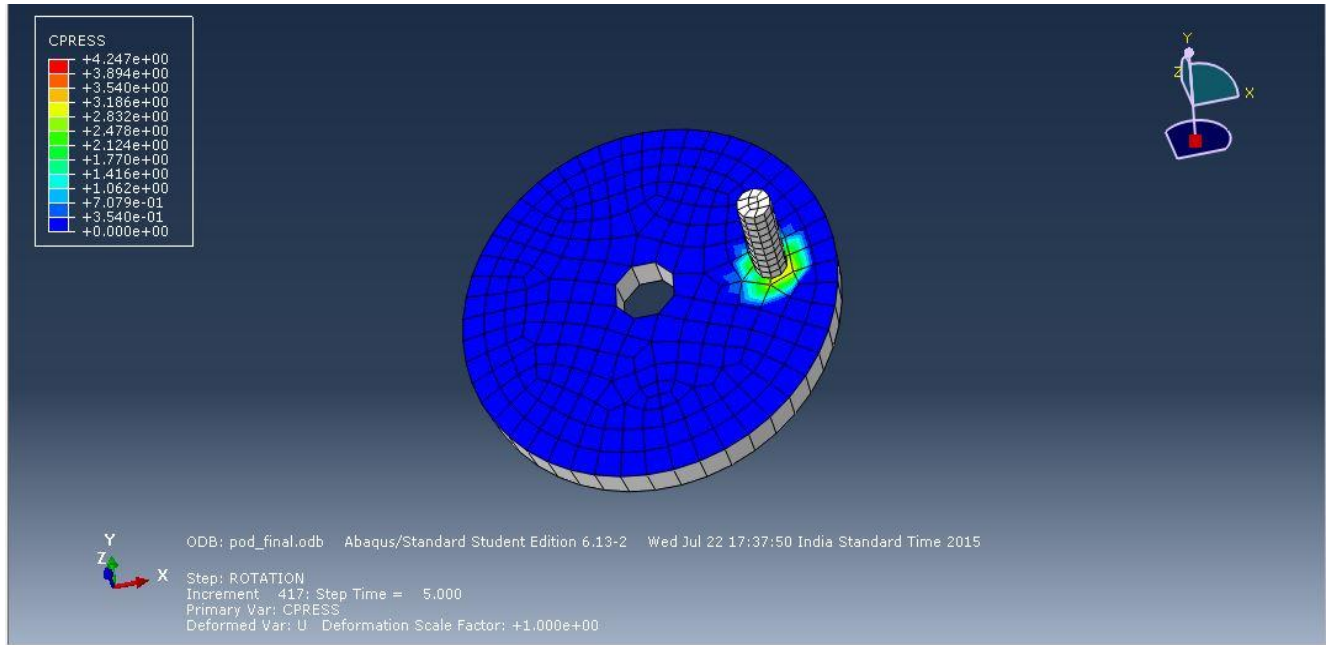Figure 4.8: Pin radius versus contact pressure graph.

Figure 4.9: Contact pressure with 2.5 radius of pin,

4.7 Effect of pin location

Pin location affects the sliding distance since it is dependent on the angular velocity. According to Archard equation wear depth is proportional to the sliding distance. Hence by varying the distance of pin form the centre will directly affects wear depth but the contact pressure remains the same due the constant angular velocity and constant applied pressure.

$$d = \omega.r.t \tag{4.2}$$

It is clear from the equation 4.2 sliding distance is proportional to the 'r' and with angular velocity and simulation time remains the constant.
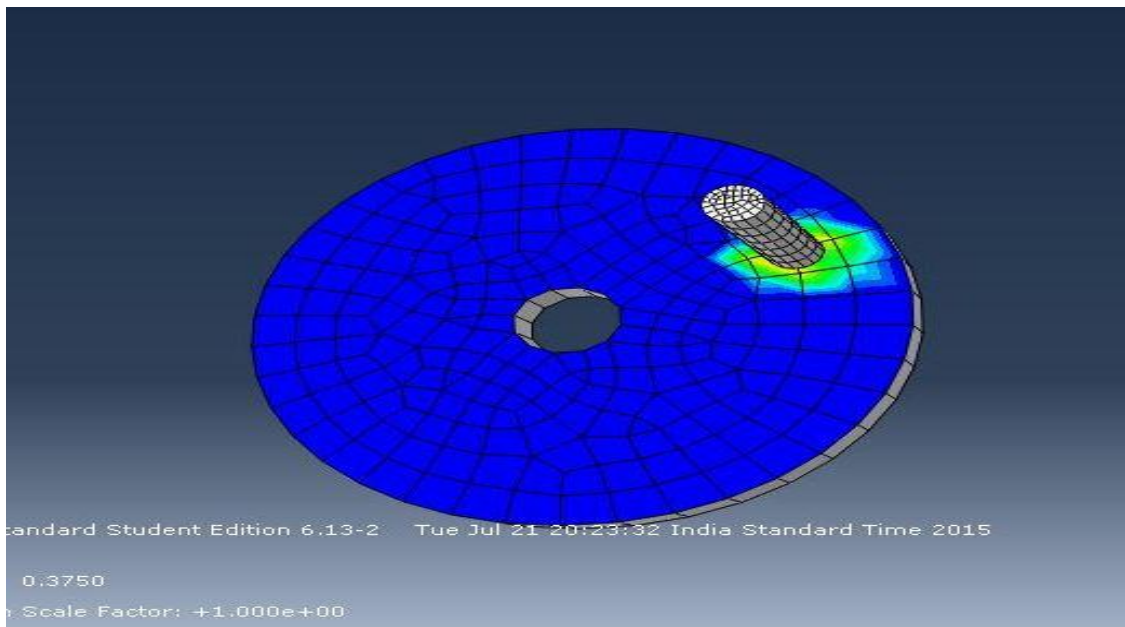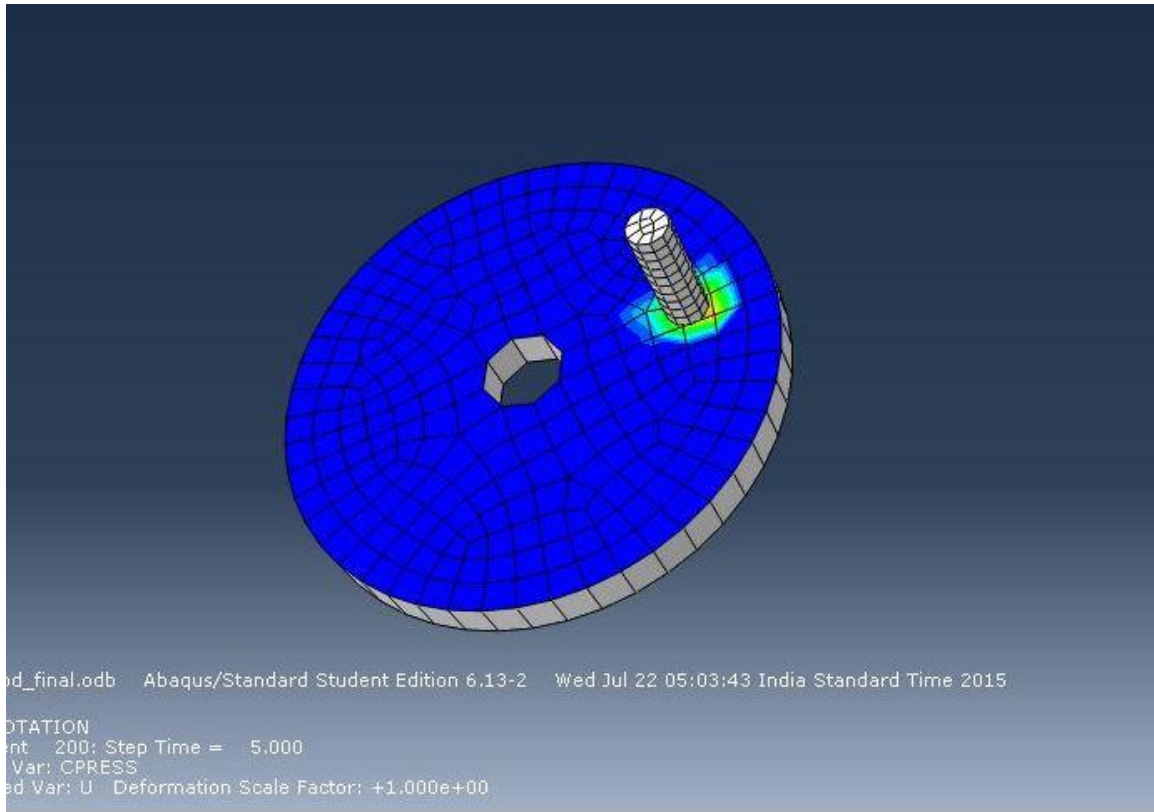
Figure 4.10: Pin at location of 20 mm and 24 mm

CHAPTER 5

CONCLUSION AND SCOPE FOR FUTURE WORK

5.1 Conclusion

In this thesis, a pin-on-disc system has been analyzed using ABAQUS CAE 6.13. The finite element model used for analyses has been updated based on experimental results from the pin-on-disc test.

- A good and reliable Pin on Disc FE model has been built. The simulations of the Pin on Disc tests give good and reliable results.
- The results out of the Finite Element model are verified with experimental results and the results are almost the same.
- The pressure distribution that has been calculated by FE program is probably good representation of the pressure distribution in real life.
- The further refinements of the models give a good more thorough view on the pressure distribution.

5.2 Scope for future work

Tribology is the vast field of science, simulation of tribological problem gives a numerical analysis of the triobological problems and real life. Following are the main future perspective of this research work:

- Different combination of pin and disc material can be explored to find out the perfect combination of matting surfaces.
- A more advance software technology can be used in future to analyze the simulation more accurately.
- Thermal analysis can also be done on future in the same problem using ABAQUS.

REFERENCES

1. ANSYS workbench user guide.

2. Podra P., Andersson, S. (1999) Simulating sliding wear with finite element method. Tribology International, 32:71-81.

3. Kim, N.H., Won, D., Burris, D., Holtkamp, B., Gessel, G.R., Swanson, P., Sawyer, W.G. (2005) Finite element analysis and experiments of metal/metal wear in oscillatory contacts. Wear, 258:1787–1793.

4. R. Bosman, D.J. Schipper, Mild wear maps for boundary lubricated contacts, Wear, Volumes 280–281, 20 March 2012, Pages 54-62, ISSN 0043-1648, http://dx.doi.org/10.1016/j.wear.2012.01.019.

5. A.R. Riahi, A.T. Alpas, Wear map for grey cast iron, Wear, Volume 255, Issues 1–6, August–September 2003, Pages 401-409, ISSN 0043-1648, http://dx.doi.org/10.1016/S0043-1648(03)00100-5

6. S.R. Pearson, P.H. Shipway, J.O. Abere, R.A.A. Hewitt, The effect of temperature on wear and friction of a high strength steel in fretting, Wear, Volume 303, Issues 1–2, 15 June 2013, Pages 622-631, ISSN 0043-1648, http://dx.doi.org/10.1016/j.wear.2013.03.048

7. C Friedrich, G Berg, E Broszeit, F Rick, J Holland, PVD CrxN coatings for tribological application on piston rings, Surface and Coatings Technology, Volume 97, Issues 1–3, December 1997, Pages 661-668, ISSN 0257-8972, http://dx.doi.org/10.1016/S0257-8972(97)00335-6.

8. E Broszeit, C Friedrich, G Berg, Deposition, properties and applications of PVD CrxN coatings, Surface and Coatings Technology, Volume 115, Issue 1, June 1999, Pages 9-16, ISSN 0257-8972, http://dx.doi.org/10.1016/S0257-8972(99)00021-3.

9. M.Y.P. Costa, M.O.H. Cioffi, H.J.C. Voorwald, V.A. Guimarães, An investigation on sliding wear behavior of PVD coatings, Tribology International, Volume 43, Issue 11,

November 2010, Pages 2196-2202, ISSN 0301-679X, http://dx.doi.org/10.1016/j.triboint.2010.07.002.

10. B Navinšek, P Panjan, I Milošev, Industrial applications of CrN (PVD) coatings, deposited at high and low temperatures, Surface and Coatings Technology, Volume 97, Issues 1–3, December 1997, Pages 182-191, ISSN 0257-8972, http://dx.doi.org/10.1016/S0257-8972(97)00393-9

11. Zhang, W.M., Meng, G. (2006) Numerical simulation of sliding wear between the rotor bushing and ground plane in micromotors. Sensors and Actuators A: Physical, 126(1):15–24.

12. Unal, H., Mimaroglu, A., Kadroglu, and Ekiz, H. (2004) Sliding Friction and Wear Behaviour of Polytetrafluoroethylene and its Composites under Dry Conditions. Material and Design, 25:239-245.

13. M.Y.P. Costa, M.O.H. Cioffi, H.J.C. Voorwald, V.A. Guimarães, An investigation on sliding wear behavior of PVD coatings, Tribology International, Volume 43, Issue 11, November 2010, Pages 2196-2202, ISSN 0301-679X, http://dx.doi.org/10.1016/j.triboint.2010.07.002.

14. Cocks, M. 'Interaction Of Sliding Metal Surfaces'. Journal of Applied Physics. Volume 33. Issue 7 (1962): 2152-2161. http://dx.doi.org/10.1063/1.1728920.

15. Morton Antler, Processes of metal transfer and wear, Wear, Volume 7, Issue 2, March–April 1964, Pages 181-203, ISSN 0043-1648, http://dx.doi.org/10.1016/0043-1648(64)90053-5.

16. https://en.wikipedia.org.

17. http://www.colorado.edu/engineering/CAS/courses.d/AFEM.d/